INTERNATIONAL ATOMIC ENERGY AGENCY
UNITED NATIONS EDUCATIONAL, SCIENTIFIC AND CULTURAL ORGANIZATION
INTERNATIONAL CENTRE FOR THEORETICAL PHYSICS
I.C.T.P., P.O. BOX 586, 34100 TRIESTE, ITALY, CABLE: CENTRATOM TRIESTE

UNITED NATIONS INDUSTRIAL DEVELOPMENT ORGANIZATION

INTERNATIONAL CENTRE FOR SCIENCE AND HIGH TECHNOLOGY
c/o INTERNATIONAL CENTRE FOR THEORETICAL PHYSICS 34100 TRIESTE (ITALY) VIA GRIGNANO, 9 (ADRIATICO PALACE) P.O. BOX 586 TELEPHONE 040-224572 TELEFAX 040-224575 TELEX 460449 APH I

SMR. 628 - 11

Research Workshop in Condensed Matter, Atomic and Molecular Physics
(22 June - 11 September 1992)

Working Party on
"DISORDERED ALLOYS"
(24 August - 4 September 1992)

" ALLOYS THEORY "

R. PRASAD
Indian Institute of Technology
Department of Physics
Kanpur 208 016
India

KKR on Random Alloys

R. Prasad
Physics Dept. IIT Kanpur

1. Introduction
2. KKR - CPA and its applications
3. Beyond the CPA

   KKR - CCPA and its applications

Collaborators: Mookerjee, Bansil
Razee & Rajput

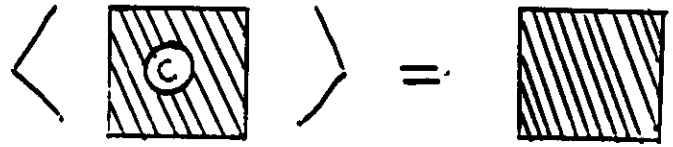

Nickel & Butler, PRL 30, 373 (73)

Motivation:
1. Beyond the CPA
2. Strong local environmental effects
3. Phase diagrams

Other approach: Embedded Cluster method

Gonis, Stocks, Butler & Winter
Phys. Rev. B 29, 555 (1984)

Generalization of CPA in tight-binding framework

1. Travelling cluster approximation

   Mills and Ratanavararaksha (78)
   Kaplan and Gray

   (i) based on diagramatic expansion
   No simple physical interpretation

   (ii) Cannot be generalized beyond two-atom clusters

2. Augmented Space Approach CCPA

   Mookerjee and co-workers

   does not have these limitations

Both methods have been proved To give positive density of states.

Razee, Mookerjee & Prasad, J. Phys: Cond. Matter 3, 3301 (1991)

Augmented Space Formalism (ASF)

Mookerjee (1973, 74)

n_i = random variable (0 or 1)

$p(\{n_i\})$ = probability distribution

$= \Pi_i \, p_i(n_i)$ for a random alloy

$$\overline{A} = \int A(\{n_i\}) \, \Pi_i \, p_i(n_i) \, dn_i$$

$$p_i(n_i) \geq 0$$

$$\int_{-\infty}^{+\infty} p_i(n_i) \, dn_i = 1$$

$P_i(E)$ = local density of states

$$= -\frac{1}{\pi} \operatorname{Im} \langle i | (E-H)^{-1} | i \rangle$$

$$P_i(E) \geq 0$$

$$\int P_i(E) \, dE = \text{finite} +$$

Recursion Method, R. Haydock (1972)

If

$$H = \begin{bmatrix} \alpha_1 & \beta_1 & 0 & 0 & \cdots \\ \beta_1 & \alpha_2 & \beta_2 & 0 & \cdots \\ 0 & \beta_2 & \alpha_3 & \beta_3 & \cdots \\ \vdots & \vdots & \vdots & \vdots & \\ \vdots & \vdots & \vdots & \vdots & \end{bmatrix}$$

Then

$$\rho_i(E) = -\frac{1}{\pi} \operatorname{Im} \cfrac{1}{E - \alpha_1 - \cfrac{\beta_1^2}{E - \alpha_2 - \cfrac{\beta_2^2}{\ddots}}}$$

$$\rho_i(n_i) = -\frac{1}{\pi} \operatorname{Im} \cfrac{1}{n_i - \alpha_1 - \cfrac{\beta_1^2}{n_i - \alpha_2 - \cfrac{\beta_2^2}{\ddots}}}$$

$$M^i = \begin{bmatrix} \alpha_1 & \beta_1 & 0 & 0 & \cdots \\ \beta_1 & \alpha_2 & \beta_2 & 0 & \cdots \\ 0 & \beta_2 & \alpha_3 & \beta_3 & \cdots \\ \vdots & \vdots & \vdots & \vdots & \\ \vdots & \vdots & \vdots & \vdots & \end{bmatrix}$$

$$\rho_i(n_i) = -\frac{1}{\pi} \operatorname{Im} \langle f_0^i | (n_i I - M^i)^{-1} | f_0^i \rangle$$

Example: Consider a binary alloy $A_x B_y$

$$n_i = 1 \quad \text{if} \quad i = A$$
$$= 0 \quad \text{if} \quad i = B$$

$$\rho_i(n_i) = x\,\delta(n_i - 1) + y\,\delta(n_i)$$

$$= -\frac{1}{\pi} \operatorname{Im} \left[\frac{x}{n_i + i0 - 1} + \frac{y}{n_i + i0} \right]$$

$$= -\frac{1}{\pi} \operatorname{Im} \left[\frac{n_i - y}{n_i (n_i - 1)} \right]$$

$$= -\frac{1}{\pi} \operatorname{Im} \left[\frac{1}{n_i - x - \cfrac{xy}{n_i - y}} \right]$$

By comparing $\alpha_1 = x \quad \alpha_2 = y$

and $\beta_1 = \sqrt{xy}$

$$\therefore \quad M^i = \begin{bmatrix} x & \sqrt{xy} \\ \sqrt{xy} & y \end{bmatrix}$$

Eigenvalues = 0, 1 Eigenvectors $|0\rangle$, $|1\rangle$

The basis in which M^i is tridiagonal

$$|f_0^i\rangle = [|0\rangle + |1\rangle]/\sqrt{2}$$
$$|f_1^i\rangle = [|0\rangle - |1\rangle]/\sqrt{2}$$

} span a 2×2 sbau ϕ_i

Augmented space Theorem

$$\bar{A} = \int A(\{n_i\})\, \Pi_i\, P_i(n_i)\, dn_i$$

$$= \langle F | \tilde{A}(\{M^i\}) | F \rangle$$

where $|F\rangle = \Pi_i |f_o^i\rangle$, represents a state in the configuration space $\phi = \Pi_i \phi_i$

Partition Theorem (Folding Th.)

$$D = \begin{bmatrix} D_I & D' \\ D'^T & D_{II} \end{bmatrix}$$

$$(D^{-1})_c = [\, D_I - D' D_{II}^{-1} D'^T \,]^{-1}$$

A. Mookerjea, in Electronic Band structure its applications (Springer Verlag, Berlin, 87)

Tight-binding CPA

$$H = \sum_i \epsilon_i P_i + \sum_{\substack{ij \\ i \neq j}} V_{ij}\ T_{ij}$$

$P_i = |i\rangle\langle i|$ $\quad T_{ij} = |i\rangle\langle j|$

No off-diagonal disorder

$\epsilon_i = \epsilon_A \quad n_i = 1$

$\epsilon_i = \epsilon_B \quad n_i = 0$

$$\epsilon_i = \epsilon_A n_i + \epsilon_B (1 - n_i)$$

$$= \epsilon_B + \delta\epsilon\, n_i \qquad \delta\epsilon = \epsilon_A - \epsilon_B$$

$$H = \epsilon_B + \delta\epsilon \sum_i P_i n_i + \sum_{ij}{}' V_{ij}\ T_{ij}$$

$$\tilde{H} = \epsilon_B \otimes I + \delta\epsilon \sum_i P_i \otimes M^i + \sum_{ij}{}' V_{ij}\, T_{ij} \otimes I$$

I, M_i operators in the configuration space

$\tilde{H}$ operator in Augmented space $\mathcal{H} \otimes \phi$

$$G_{oo}(z) = \langle o | (z - H)^{-1} | o \rangle$$

By Augmented space Theorem

$$\langle G_{oo}(z) \rangle = \langle o, F | (z - \tilde{H})^{-1} | F, o \rangle$$

$$|F\rangle = \pi_i |f_o^i\rangle$$

$$\tilde{H} = \begin{pmatrix} H_I & H' \\ H'^T & H_{II} \end{pmatrix}$$ ← corresponds to N-1 sites

$$H_I = \epsilon_B \otimes I + \delta\epsilon \, P \otimes_A M^o$$

$$H_I = \begin{pmatrix} \bar{\epsilon} & W \\ W & \tilde{\epsilon} \end{pmatrix}$$

$$W = \sqrt{xy}\,\delta\epsilon$$

$$\bar{\epsilon} = x\epsilon_A + y\epsilon_B$$

$$\tilde{\epsilon} = y\epsilon_A + x\epsilon_B$$

$$H_{II} = \left(\sigma_o \sum_{i \neq o} P_i + \sum_{\substack{i \neq o \\ j \neq o}}{}' V_{ij} T_{ij} \right) \otimes |F\rangle\langle F|$$

Five lines

$$H' = \left(\sum_{j \neq o} V_{oj} T_{oj} \right) \otimes |F_s\rangle\langle F|$$

By partitioning

$$[(z - \tilde{H})^{-1}]_I = (z - \hat{H})^{-1}$$

$$\hat{H} = H_I + H'(z - H_{II})^{-1} H'^T = \begin{pmatrix} H_1 & H_{12} \\ H_{21} & H_2 \end{pmatrix}$$

$$= \begin{pmatrix} \bar{\epsilon} + A & W \\ W & \tilde{\epsilon} + A \end{pmatrix} \qquad A = \sum_{\substack{j \neq o \\ k \neq o}} V_{oj} G^o_{jk} V_{ko}$$

G^o = GF of the system with o'th site removed.

Need only $\langle o, f_o | (z - \hat{H})^{-1} | o, f_o \rangle$ element

Another partitioning

$$\langle G_{oo} \rangle = \langle o, f_o | (z - \hat{H})^{-1} | o, f_o \rangle$$

$$= \langle o | (z - \hat{H}')^{-1} | o \rangle$$

$$\hat{H}' = H_1 + H_{12} G_2 H_{21}$$

Effective medium

$$H_{eff} = \sigma_0 \sum_i P_i + \sum_{ij}{}' V_{ij}\, T_{ij}$$

$$= \begin{pmatrix} \sigma_0 & \vdots & \\ \cdots & \sigma_0 & \cdots \\ & \vdots & \ddots \end{pmatrix}$$

$$G_{00}^{eff} = \left[z - \sigma_0 - \sum_{\substack{j \neq 0 \\ k \neq 0}} V_{0j}\, G^0_{jk}\, V_{k0} \right]^{-1}$$

Now $\langle G_{00} \rangle = G_{00}^{eff}$

$$\sigma_0 = \bar{\epsilon} + \frac{W^2\, G_{00}}{1 - [(y-x)\delta\epsilon + (\bar{\epsilon} - \sigma_0)] G_{00}}$$

Same as obtained by multiple scattering theory.

KKR - CCPA

Green's function for a system of muffin-tin potentials (Faulkner & Stocks Phys. Rev. B 21, 3222 (80)

$$G(\vec{r}, \vec{r}'; E) = \sum_{LL'} Z_L^i(\vec{r}_i)\, T_{LL'}^{ij}\, Z_{L'}^j(\vec{r}_j') - \delta_{ij} \sum_L Z_L^i(\vec{r}_i)\, J_L^i(\vec{r}_j')$$

$\vec{r}$ lies in i^{th} cell
$\vec{r}'$ " j^{th} "

$$T^{ij} = (A^{-1})^{ij} = [(\tau^{-1} - B)^{-1}]^{ij}$$

$$A^{ij}_{LL'} = c^i_{LL'}\, \delta_{ij} - B^{ij}_{LL'}$$

$$c^i = \tau_i^{-1}$$

$$= c^A n_i + c^B (1 - n_i)$$

$$= c^B + \delta c\, n_i$$

$$\delta c = c^A - c^B$$

$$A = \sum_i c^i |i\rangle\langle i| - \sum_{i \neq j} B^{ij} |i\rangle\langle j|$$

$$= c^B + \delta c \sum_i |i\rangle\langle i|\, n_i - \sum_{i \neq j} B^{ij} |i\rangle\langle j|$$

By Augmented space theorem

$$\langle T^{ij} \rangle = \langle i, F | \tilde{A}^{-1} | j, F \rangle$$

$$\tilde{A} = c^B \otimes I + \delta c \sum_i |i\rangle\langle i| \otimes M^i - \sum_{i \neq j} B^{ij} |i\rangle\langle j| \otimes I$$

I and M^i, operators in the configuration space ϕ

$\tilde{A}$ is a operator in Augmented space $\psi = \mathcal{H} \otimes \phi$ where $\mathcal{H}$ is the Hilbert space spanned by $|i\rangle$.

The Augmented space is spanned by $|i, F_s\rangle$ and its rank is $N \times 2^N$.

Restricted site averages

$$\langle T^{ii} \rangle_\alpha = D^\alpha T^{ii}_{eff}$$

$$\langle T^{ij} \rangle_{\alpha\beta} = D^\alpha T^{ij}_{eH} D^\beta$$

$$D^\alpha = [I + (c^\alpha - c_{eH}) T^{oo}_{eH}]^{-1}$$

Partition the augmented space ψ into Two subspaces I and II $\quad m \times 2^m$

I spanned by $\{|i, F_s\rangle\}$ $i \in C$ (cluster)

II Remaining subspace C', rank $(N-m) \times 2^m$

Approximation: replace subspace II by an effective medium

$$\tilde{A} = \begin{bmatrix} A_I & A' \\ A'^T & A_{II} \end{bmatrix}$$

by partition theorem

$$[\tilde{A}^{-1}]_I = [A_I - A' A_{II}^{-1} A'^T]^{-1} = \hat{A}^{-1}$$

$$A_I = c^B \sum_{i \in C} |i\rangle\langle i| \otimes \sum_{F_s \in \phi} |F_s\rangle\langle F_s| + \delta c \sum_{i \in C} |i\rangle\langle i| \otimes M^i - \sum_{\substack{i,j \in C \\ i \neq j}} B^{ij} |i\rangle\langle j| \otimes \sum_{F_s} |F_s\rangle\langle F_s|$$

$$A_{II} = \Big[c_{eff} \sum_{k \in C'} |k\rangle\langle k| - \sum_{\substack{k,l \in C' \\ k \neq l}} B^{kl}_{eff} |k\rangle\langle l| \Big] \otimes \sum_F |F\rangle\langle F|$$

$\pi_d f_o^i \rangle$

$$A' = -\Big[\sum_{\substack{i \in C \\ k \in C'}} B^{ik}_{eff} |i\rangle\langle k| \Big] \otimes \sum_{F_s} |F_s\rangle\langle F_s|$$

$$A' A_{II}^{-1} A'^T = \sum_{i,j \in C} \mathcal{E}_C^{ij} |i\rangle\langle j| \otimes \sum_{F_s} |F_s\rangle\langle F_s|$$

$$\mathcal{E}_C^{ij} = \sum_{k,l \in C'} B^{ik}_{eff} T^{(c)kl}_{eH} B^{lj}_{eff}$$

$$B^{kl}_{eH} = B^{kl} + b^{kl} \leftarrow \text{off-diagonal correction to } C$$

$$T^c_{eH} = A_{II}^{-1}$$

$$\hat{A} = \Big[\sum_{i \in C} (c^B - \mathcal{E}_C^{ii}) |i\rangle\langle i| - \sum_{\substack{i,j \in C \\ i \neq j}} (B^{ij} + \mathcal{E}_C^{ij}) \times |i\rangle\langle j| \Big] \otimes \sum_{F_s} |F_s\rangle\langle F_s| + \delta c \sum_{i \in C} |i\rangle\langle i| \otimes M^i$$

Again partition $\hat{A}$ (rank $m \times 2^m$) as

$$\hat{A} = \begin{bmatrix} A_1 & A_{12} \\ A_{21} & A_2 \end{bmatrix}$$

Subspace 1 : spanned by $|i, F\rangle$, $i \in C$
rank = m

subspace 2 : Remaining subspace
rank $m \times (2^m - 1)$

$$\big[\hat{A}^{-1}\big]_1 = \big[A_1 - A_{12} A_2^{-1} A_{21}\big]^{-1}$$

$$A_1 = \sum_{i \in C} (\bar{C} - \mathcal{E}_C^{ii}) |i\rangle\langle i| - \sum_{\substack{i,j \in C \\ i \neq j}} (B^{ij} + \mathcal{E}_C^{ij}) |i\rangle\langle j|$$

$$\bar{C} = x C^A + y C^B$$

From augmented space theorem

$$\langle T^{ij} \rangle = \langle i | (A_1 - A_{12} A_2^{-1} A_{21} | j \rangle \quad i,j \in C$$

$$A_{eH} = C_{eH} \sum_i |i\rangle\langle i| - \sum_{\substack{i,j \\ i \neq j}} B^{ij}_{eH} |i\rangle\langle j|$$

$$T^{ij}_{eH} = \langle i | A_{eH}^{-1} | j \rangle$$

$$A_{eff} = \sum_{atoms} \left[A^{T} A^{0}_{eff} \right]$$

By partitioning technique

$$T^{ij}_{eff} = \langle i | \left[\sum_{k \in C} (c_{eff} - \mathcal{Q}^{kk}_{c}) |k\rangle\langle k| - \sum_{\substack{k,l \in C \\ k \neq l}} (B^{kl}_{eff} + \mathcal{Q}^{kl}_{c}) |k\rangle\langle l| \right]^{-1} | j \rangle$$

Self-consistency condition

$$\langle T^{ij} \rangle = T^{ij}_{eff}$$

$$A_1 - A_{12} A_2^{-1} A_{21} = \sum_{i \in C} (c_{eff} - \mathcal{Q}^{ii}_{c}) |i\rangle\langle i| - \sum_{i,j \in C} (B^{ij}_{eff} + \mathcal{Q}^{ij}_{c}) |i\rangle\langle j|$$

$\Rightarrow$ KKR-CCPA equations

$$c_{eff} = \bar{c} - \langle i | A_{12} A_2^{-1} A_{21} | i \rangle$$

$$b^{ij} = \langle i | A_{12} A_2^{-1} A_{21} | j \rangle \quad \text{for } i \neq j$$

$$b^{ji} = (b^{ij})^{T}$$

No. of self consistent eqns $= m\frac{(m-1)}{2} + m$

$$\rho(E) = -\frac{1}{\pi} \operatorname{Im} \int_{\Omega} \langle G(\vec{r}, \vec{r}; E) \rangle \, d^3 r$$

$$= -\frac{1}{\pi} \operatorname{Tr} \operatorname{Im} \left[x F^{A} D^{A} + y F^{B} D^{B} \right] T^{00}_{eff}$$

$$F^{\alpha} = \int_{\Omega} F^{\alpha}(\vec{r}_n, \vec{r}_n) \, d^3 r_n$$

$$F^{\alpha}_{LL'}(\vec{r}_n, \vec{r}_n') = Z^{n}_{L}(\vec{r}_n) \, Z^{n}_{L'}(\vec{r}_n')$$

$$\rho^{\alpha}(E) = -\frac{1}{\pi} \operatorname{Tr} \operatorname{Im} F^{\alpha} D^{\alpha} T^{00}_{eff}$$

$$\rho^{\alpha}(\vec{r}) = -\frac{1}{\pi} \operatorname{Tr} \operatorname{Im} \int_{-\infty}^{E_F} F^{\alpha}(\vec{r}, \vec{r}) D^{\alpha} T^{00}_{eff} \, dE$$

Full charge-self consistent calculation

Razee & Prasad, Phys. Rev. B 45, 3265 (92)

Application to 1 D Alloy Model

W. H. Butler, Phys. Rev. B 14, 468 (76).

$$H = -\frac{d^2}{dx^2} + \sum_n v_n(x - na)$$

a = interatomic spacing

$v_n(x) = 0$ for $|x| \geq r_{MT} \leq a$

Only two ℓ values 0, 1

$$\tau_\ell = -\kappa\, e^{i\theta_\ell} \sin\theta_\ell$$

$$\mathrm{Im}\, G^{SD}(x,x') = \sum_{\ell\ell'} Z_\ell(x)\, \mathrm{Im}\, T^{00}_{\ell\ell'}\, Z_{\ell'}(x')$$

$B(\vec{k}, E)$ can be found analytically.

Cluster of 2 atoms

$$v_n(x) = -V_0^{A(B)} \qquad x \leq r_{MT}$$

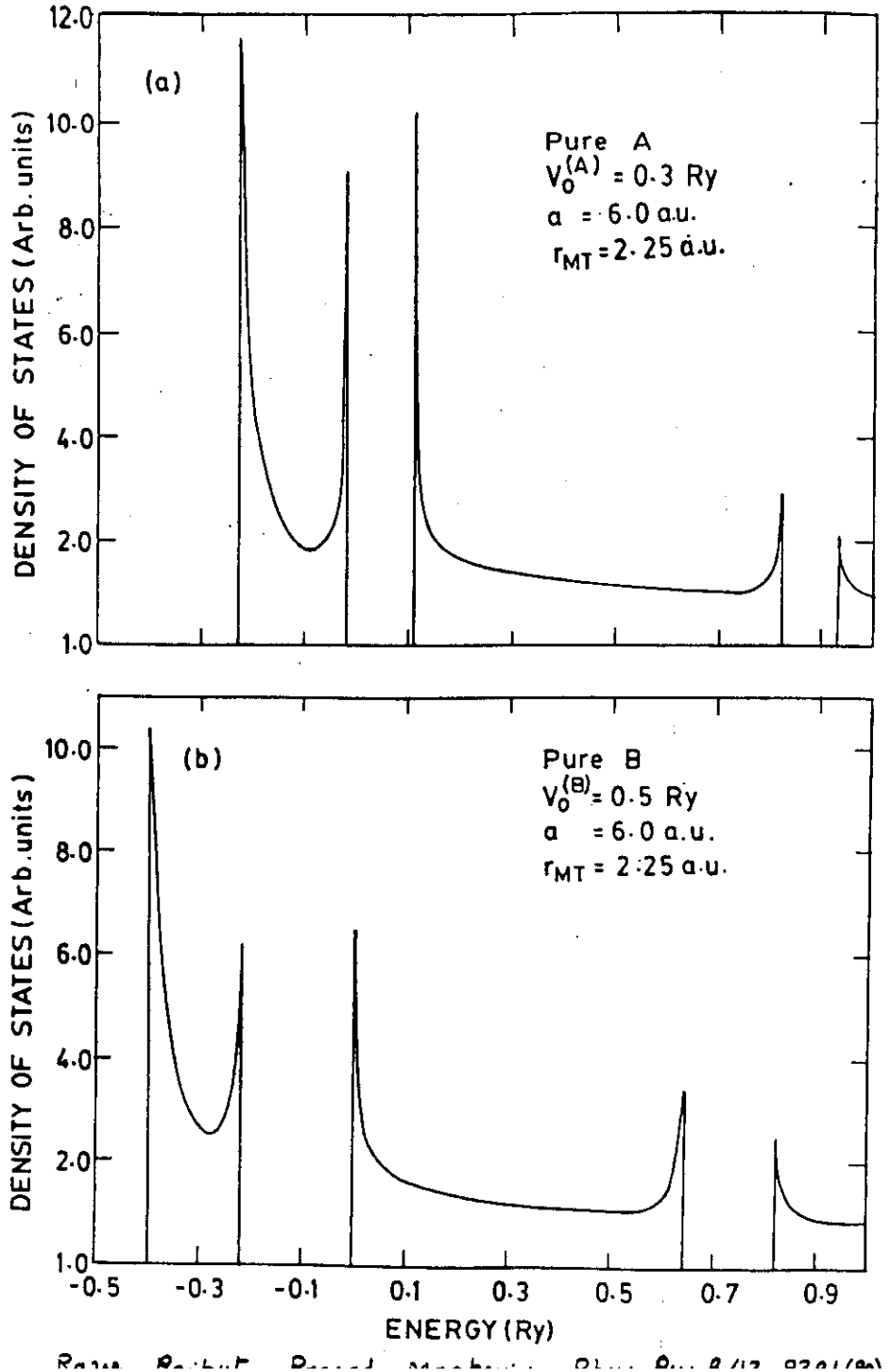

Local Density of states

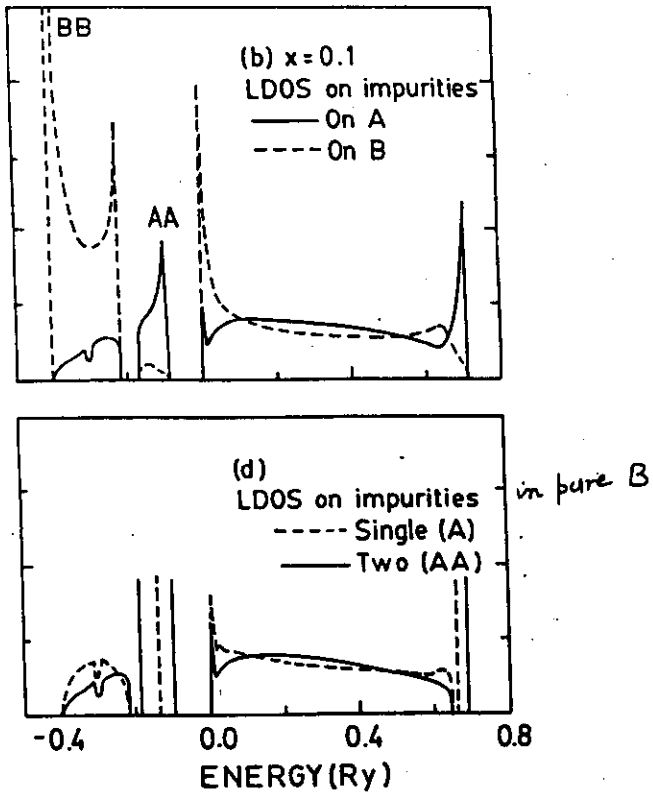

Razee, Rajput, Prasad, Mookerjee, Phys. Rev. B (90)

Density of states

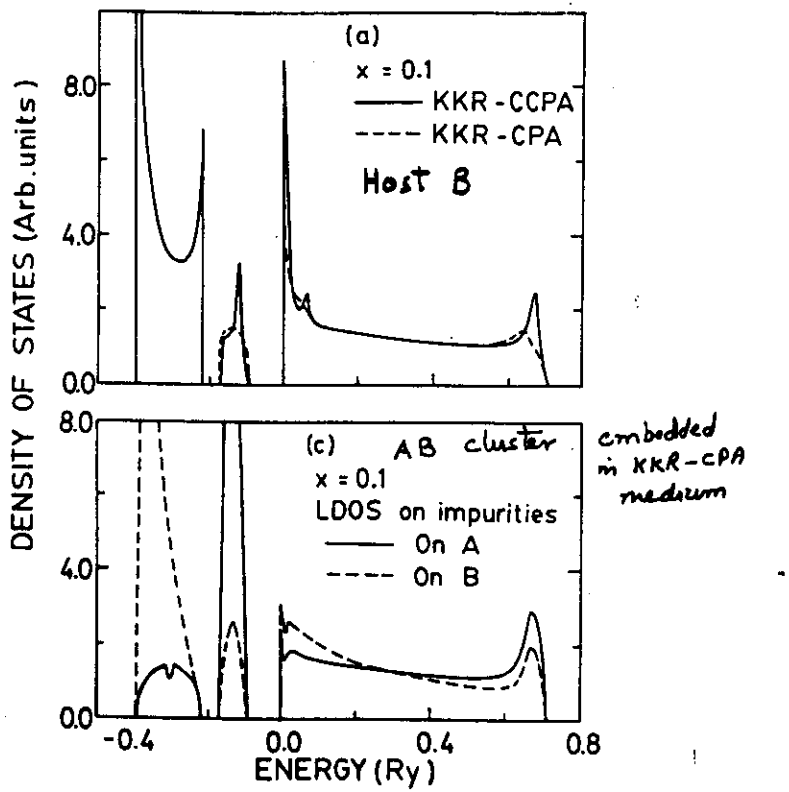

Razee, Rajput, Prasad, Mookerjee, Phys. Rev B (90)

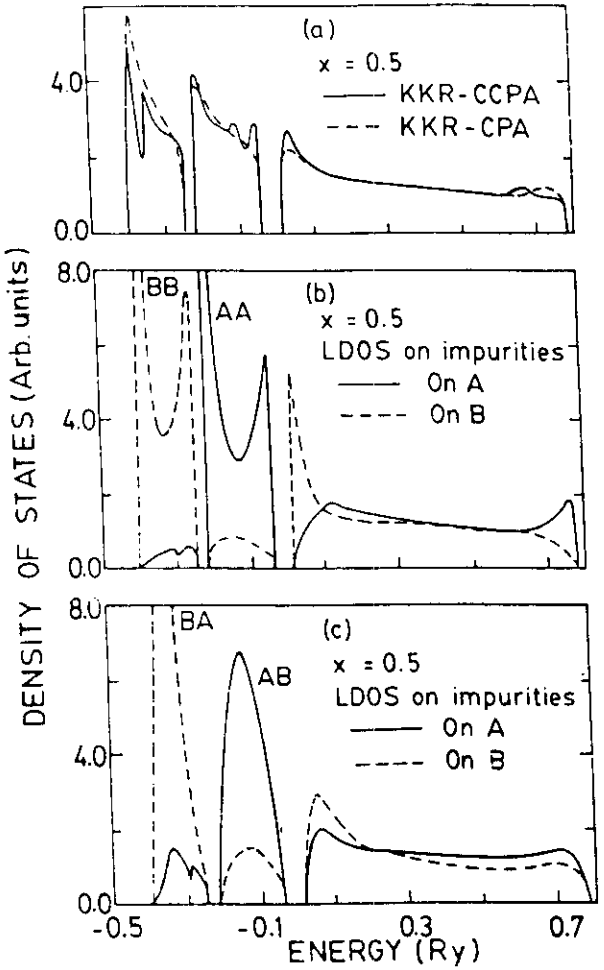
(a)
x = 0.5
KKR-CCPA
KKR-CPA
4.0
0.0
8.0
BB
AA
(b)
x = 0.5
LDOS on impurities
On A
On B
4.0
0.0
8.0
BA
AB
(c)
x = 0.5
LDOS on impurities
On A
On B
4.0
0.0
-0.5
-0.1
0.3
0.7
ENERGY (Ry)
DENSITY OF STATES (Arb. units)

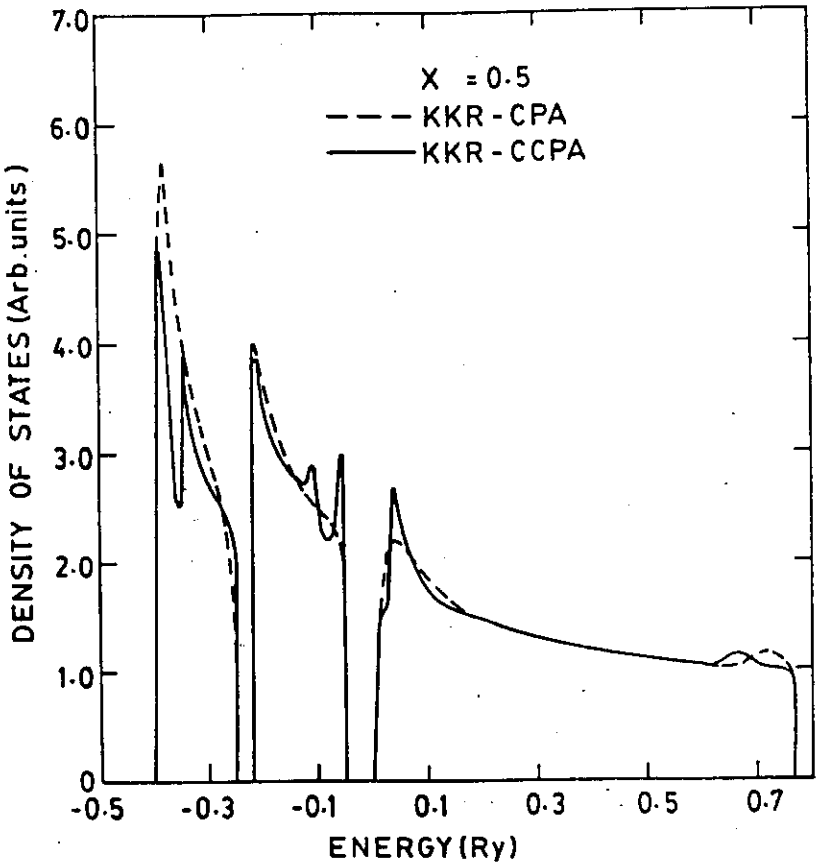
X = 0·5
KKR-CPA
KKR-CCPA
7.0
6.0
5.0
4.0
3.0
2.0
1.0
0
-0.5
-0.3
-0.1
0.1
0.3
0.5
0.7
ENERGY (Ry)
DENSITY OF STATES (Arb. units)

Embedded Cluster Method

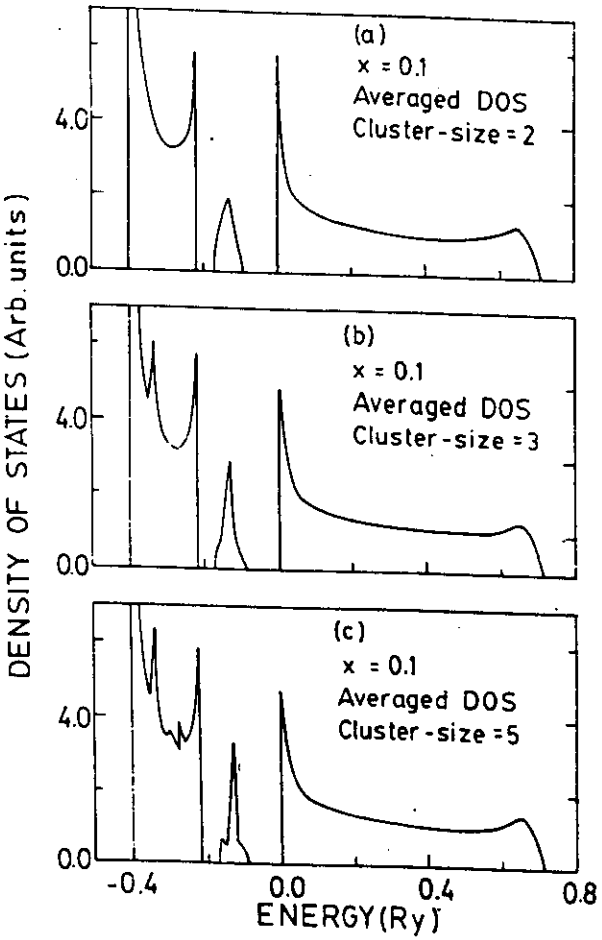

Razee, Rajput, Prasad, Mookerjee, Phys. Rev. B (90)

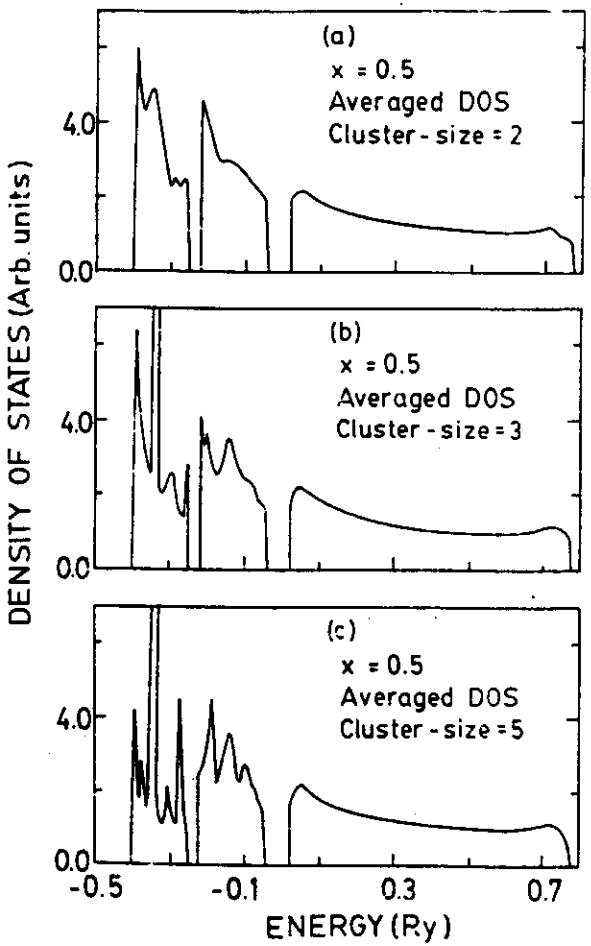

Application to s-phase shift semicircular model

P. Soven, Phys. Rev B 2, 4715 (70).

$$c = \cot \delta_0^{A(B)} = \frac{E_{A(B)} - E}{\Gamma_{A(B)}} \qquad \ell = 0 \text{ only}$$

$E_{A(B)}$ = resonant energy

$\Gamma_{A(B)}$ = resonance half-width

$$\tilde{B}_{\vec{q}} = \frac{B_{\vec{q}}}{\chi} - i$$

$B_{\vec{q}}$ ← KKR str. fn.

has no energy dependence

$$t^{-1} = -\chi c + i$$

$$T_{00} = -\frac{1}{\chi N} \sum_{q} (c + \tilde{B}_{\vec{q}})^{-1}$$

$$= -\frac{1}{\chi} \int (c+b)^{-1} f^{0}(b)\, db$$

$$f^{0}(b) = \frac{1}{N} \sum_{q} \delta(b - \tilde{B}_{\vec{q}})$$

which is chosen

$$f^{0}(b) = \frac{2}{\pi} (1-b^2)^{1/2} \qquad |b| \le 1$$

$$= 0 \qquad\qquad |b| > 1$$

Then

$$T_{00} = -\frac{1}{\chi} g_{00}$$

$$g_{00} = 2\left[c + (c^2-1)^{1/2}\right]$$

Similarly

$$T_{01} = -\frac{1}{\chi} \int f'(b) (c+b)^{-1} db$$

$$f'(b) = \frac{1}{N} \sum_{q} e^{-i \vec{q} \cdot \vec{R}_{01}} \delta(b - \tilde{B}_{\vec{q}})$$

which is chosen as

$$f'(b) = -\frac{\lambda}{\pi} (1-b^2)^{1/2} b \qquad |b| \le 1$$

$$= 0 \qquad\qquad |b| > 1$$

$$T_{01} = -\frac{1}{\chi} \frac{\lambda}{8} g_{00}^2$$

There is one-to-one correspondence between KKR-CCPA equations for this model and TB-CCPA equations for the analogous semicircular model

Rajput, Razee, Prasad and Mookerjee, J. Phys. Condensed Matter (1989)

$X = .5$

$E_A = -E_B = 0.5$

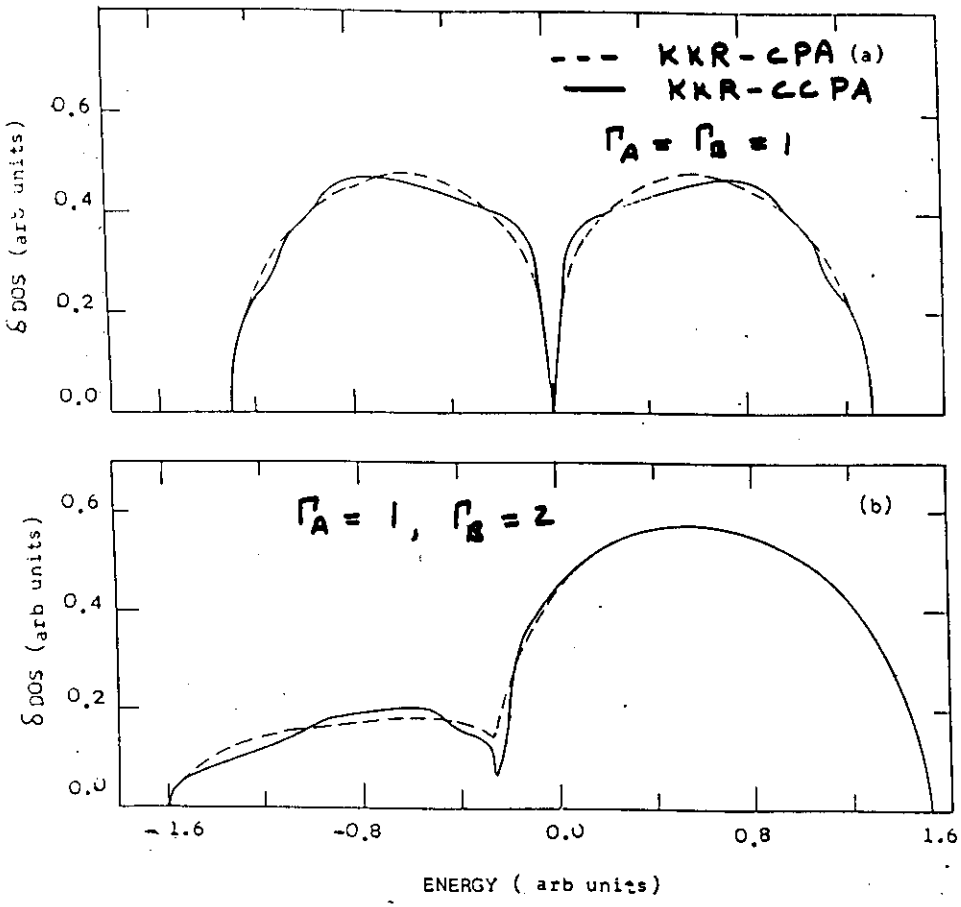

Figure 7

Conclusion

1. We have combined KKR and ASF methods to go beyond the CPA.
2. KKR-CCPA density of states shows rich structure arising from correlated scattering from clusters of atoms in the effective medium.
3. We have shown that one-to-one correspondence exists between KKR-CCPA equations for the s-phase shift model and TB-CCPA equations for the analogous semicircular model.

Electronic structure of disordered alloys: Korringa-Kohn-Rostoker cluster coherent-potential approximation

S. S. A. Razee, S. S. Rajput, R. Prasad, and A. Mookerjee*
Department of Physics, Indian Institute of Technology, Kanpur 208016, India
(Received 21 February 1989; revised manuscript received 3 July 1990)

A self-consistent cluster theory, the Korringa-Kohn-Rostoker cluster coherent-potential approximation (KKR-CCPA), is presented to study the electronic structure of the random, substitutionally disordered metallic alloys. This theory combines the augmented-space formalism and conventional Korringa-Kohn-Rostoker methods to determine the effective medium self-consistently. One advantage of this method is that it preserves Herglotz properties of the configuration-averaged Green's function needed to calculate various electronic properties, such as charge densities, essential for full charge self-consistency. Unlike the single-site approximations, the KKR-CCPA introduces diagonal as well as off-diagonal corrections in the scattering matrices. The formulation has been applied to a model one-dimensional alloy. We find that the density of states in the KKR-CCPA is somewhat structured, due to correlated scattering from clusters of atoms.

I. INTRODUCTION

Most of the current studies on electronic properties of random substitutionally disordered metallic alloys are done within single-site approximations, in which the real disordered system is replaced by a translationally symmetric effective medium with an effective scatterer on each site. The effective scatterer is then determined by averaging over all the possible configurations of a single real atom embedded in the effective medium. The two most commonly used single-site approximations are the average-t-matrix approximation and the coherent-potential approximation (CPA).[1-3] In the average-t-matrix approximation, the effective scattering matrix is the average of those of the alloy constituents. In the CPA, the effective medium is determined by a self-consistency condition, which requires that the average scattering from a single real atom embedded in the effective medium be zero. It is generally agreed that the CPA is the best single-site approximation. However, it might fail whenever a single-site effective-medium description becomes inadequate, e.g., in the presence of strong local environmental effects, such as short-range order and clustering tendencies. These local environmental effects can be investigated, accurately and convincingly, only through a cluster or multisite approximation. Recent experimental works on CuPd (Refs. 4 and 5) and CuPt (Refs. 5 and 6) systems show that the CPA is not adequate for these systems.

With the realization of the need to go beyond the CPA, several attempts have been reported.[7-24] These attempts can be broadly classified into two categories: non-self-consistent cluster approaches[11-14] and self-consistent cluster approaches.[7-10,16-24] In the non-self-consistent approach, there has been a considerable amount of work within the tight-binding framework. But, to our knowledge, only the work of Gonis *et al.*[12,13] is within the conventional Korringa-Kohn-Rostoker (KKR) framework. In this work, a cluster consisting of a central site and its shell of nearest neighbors was embedded in an effective medium determined within the KKR-CPA method. The density of states (DOS) was then obtained from the site-diagonal element of the Green's function at the center of the cluster. The effective medium, however, was not determined self-consistently with respect to the cluster. It was expected that the effects of the cluster self-consistency would be small. However, the work of Stefanou *et al.*[25] on CuPd systems shows that these effects may be significant.

In the self-consistent cluster approach also, a great deal of work has been done, mostly on the tight-binding models,[7-10,16-18] though a few papers have appeared on muffin-tin models[22-24] also. Some of these approaches are either too difficult to implement computationally, such as the molecular CPA,[8] or they lack proper physical behavior.[7,9,15] Traveling cluster approximation[17] and augmented-space formalism[26,27] (ASF) are the only approaches which have been proved to be analytic, while preserving the conservation laws and sum rules.[18,28,29] The ASF, originally developed in the tight-binding framework, provides a self-consistent cluster coherent-potential approximation (CCPA) in which one can go beyond the CPA in a systematic way.[16] In this method, the effective medium is determined by the self-consistency condition that the average scattering from all the possible configurations of a real cluster embedded in the effective medium be zero. Unlike the molecular CPA, the CCPA gives a translationally invariant effective medium.[29] There is a vast literature on the ASF (Refs. 18-21 and 26-28) and it has been used extensively for electronic structure calculations in the tight-binding framework.[21]

The ideas of ASF are rather general and can be incorporated within the conventional KKR method as well.[24] Although a formula for averaged DOS using Lloyd's formula[3,30] has already been developed,[24] it does not allow the calculation of charge densities and, therefore, the

prospect of doing charge self-consistency is ruled out. Furthermore, it is now generally agreed that the electronic properties of an alloy should be calculated by the Green's-function method, as the formulas based on Lloyd's formula may give unphysical results,[30,31] such as negative DOS and negative spectral density. Our formulation is based on the Green's function and therefore overcomes these difficulties: using it one can calculate charge density and therefore can achieve charge self-consistency within the local-density approximation of the density-functional theory.

This theory can also treat a random ternary alloy. Work within the tight-binding framework has already been reported.[32] An extension of the theory to deal with nonrandom effects like short-range order has also been reported in the tight-binding framework.[33] We have extended it using the KKR framework and our calculations are in progress. Therefore we plan to discuss the nonrandom effects in a separate paper.

The outline of the paper is as follows. We present our formulation in Sec. II. In Sec. II A we briefly discuss the main ideas of the ASF. In Sec. II B we combine the ASF and the conventional KKR method to formulate the KKR-CCPA formalism. It is found that the KKR-CCPA introduces diagonal as well as off-diagonal corrections in the scattering matrices of the effective medium. In Appendix A we present simplification of the KKR-CCPA equations for clusters of one atom and two atoms. We also show that, for a one-atom cluster, the KKR-CCPA equations reduce to the familiar KKR-CPA equation, which is the correct limit. In Sec. II C we give the expressions for the configuration-averaged Green's function and various quantities which can be obtained from it, such as DOS and charge densities. The problem of impurities embedded in the effective medium has also been discussed in this section. As a first attempt to implement KKR-CCPA, we have applied it to a one-dimensional model alloy as presented in Appendix B. This model is chosen because it has analytical expressions for various quantities[34] and thus is computationally simpler. In Sec. III we present the results of our calculations of DOS within KKR-CPA and KKR-CCPA. We also present local DOS on impurities for a cluster of two real impurities embedded in the KKR-CPA medium. We compare the KKR-CCPA DOS with these local DOS's on the impurities and show that their features are correlated. This suggests that the structures in the KKR-CCPA DOS are due to correlated scattering from the clusters of atoms. We also present the averaged DOS on the central site of a cluster of atoms embedded in the KKR-CPA medium, for clusters of two, three, and five atoms. These calculations are similar to the embedded cluster calculations of Gonis *et al.*[13] We find that this averaged DOS reproduces some of the structures of the KKR-CCPA DOS, which become prominent as we increase the cluster size.

II. FORMULATION

A. The augmented-space formalism

The ASF (Refs. 26 and 27) is an efficient and convenient method for configuration averaging a quantity, which is a function of a set of random variables $\{n_i\}$, provided the probability distribution $p(\{n_i\})$ is known explicitly. The configuration average of a function $\underline{A}(\{n_i\})$ is the integral

$$\langle \underline{A} \rangle = \int \underline{A}(\{n_i\}) p(\{n_i\}) \prod_i dn_i \ . \tag{2.1}$$

For a random substitutional alloy with no short-range order, the composite probability distribution $p(\{n_i\})$ can be written as a product of the individual single-site probability distributions $p_i(n_i)$, i.e.,

$$p(\{n_i\}) = \prod_i p_i(n_i) \ . \tag{2.2}$$

If we assume that $p_i(n_i)$ has finite moments to all orders, then it is always possible to write $p_i(n_i)$ as the matrix element[26]

$$p_i(n_i) = -\frac{1}{\pi} \mathrm{Im} \langle f_0^{(i)} | (n_i \underline{I} - \underline{M}^{(i)})^{-1} | f_0^{(i)} \rangle \ , \tag{2.3}$$

where $\underline{M}^{(i)}$ is an operator in the configuration space ϕ_i of rank m, spanned by $\{|f_j^{(i)}\rangle\}$, $j=0,1,2,\ldots,m-1$, with m being the number of components of the alloy. The configuration space ϕ_i contains all the possible configurations for the site i and $|f_0^{(i)}\rangle$ is referred to as the ground state in ϕ_i. The basis $\{|f_j^{(i)}\rangle\}$ can be defined if $p_i(n_i)$ is known explicitly. For a random binary alloy A_xB_y, $p_i(n_i)$ can be written as

$$p_i(n_i) = x\delta(n_i - 1) + y\delta(n_i) \ ,$$

where

$$n_i = \begin{cases} 1 & \text{for } i = A \\ 0 & \text{for } i = B \ . \end{cases} \tag{2.4}$$

It immediately follows from Eq. (2.4) that $p_i(n_i)$ satisfies the required conditions, namely,

$$\int p_i(n_i) n_i^l dn_i \text{ finite for } l = 0,1,2,\ldots$$

and

$$p_i(n_i) \geq 0 \ . \tag{2.5}$$

For $p_i(n_i)$ as defined in Eq. (2.4), $\underline{M}^{(i)}$ is a tridiagonal matrix in the space ϕ_i of rank 2 spanned by $|f_0^{(i)}\rangle$ and $|f_1^{(i)}\rangle$ with a representation[26]

$$\underline{M}^{(i)} = \begin{bmatrix} x & \sqrt{xy} \\ \sqrt{xy} & y \end{bmatrix} . \tag{2.6}$$

It is easily seen that

$$\underline{M}^{(i)} |f_0^{(i)}\rangle = x |f_0^{(i)}\rangle + \sqrt{xy} \, |f_1^{(i)}\rangle \ ,$$

and

$$\underline{M}^{(i)} |f_1^{(i)}\rangle = y |f_1^{(i)}\rangle + \sqrt{xy} \, |f_0^{(i)}\rangle \ .$$

The bases $|f_0^{(i)}\rangle$ and $|f_1^{(i)}\rangle$, referred to as the ground state and the excited state in the configuration space, respectively, are given by

$$|f_0^{(i)}\rangle = \sqrt{x} \, |\mathcal{A}\rangle_i + \sqrt{y} \, |\mathcal{B}\rangle_i$$

and

$$|f_1^{(i)}\rangle = \sqrt{y}\,|\mathcal{A}\rangle_i - \sqrt{x}\,|\mathcal{B}\rangle_i \ . \tag{2.7}$$

The bases $|\mathcal{A}\rangle_i$ and $|\mathcal{B}\rangle_i$ indicate the occupancy of the ith site. By the augmented-space theorem[26] we get

$$\langle \underline{A} \rangle = \langle F|\tilde{\underline{A}}(\{\underline{M}^{(i)}\})|F\rangle \ , \tag{2.8}$$

where $|F\rangle = \prod_i |f_0^{(i)}\rangle$ and represents a state in the configuration space $\Phi = \prod_i \phi_i$. The remaining bases in the configuration space are those for which there are excited states $|f_1^{(i)}\rangle$ on one or more sites. These are conventionally written as $|F_s\rangle$, where s is a composite index of one or more sites on which we have $|f_1^{(i)}\rangle$, while on the rest of the sites we have $|f_0^{(i)}\rangle$. For example, a state $|F_{jk\ldots l}\rangle$ is given by

$$|F_{jk\ldots l}\rangle = \prod_i |f_n^{(i)}\rangle \text{ with } n = \begin{cases} 0 & \text{for } i \neq j,k,\ldots,l \\ 1 & \text{for } i = j,k,\ldots,l \ . \end{cases} \tag{2.9}$$

$\tilde{\underline{A}}(\{\underline{M}^{(i)}\})$ is an operator in the augmented space $\psi = \mathcal{H} \otimes \Phi$, where $\mathcal{H}$ is the Hilbert space spanned by $\{|i\rangle\}$. The augmented space is spanned by $\{|i,F_s\rangle\}$ and its rank is $N \times 2^N$, where N is the total number of atoms in the solid. The operator function $\tilde{\underline{A}}(\{\underline{M}^{(i)}\})$ is the same function of $\{\underline{M}^{(i)}\}$ as $\underline{A}(\{n_i\})$ is of $\{n_i\}$.[26] Note that Eq. (2.8) is exact, but cannot be used for computational purposes. Therefore we look for some approximation which will reduce the rank of the augmented space. The simplest approximation is the CCPA, in which a small cluster $\mathcal{C}$ is chosen out of $\{i\}$ and the complement of the cluster is taken as an effective medium. The randomness comes only within $\mathcal{C}$ and so the configuration averaging is done over all the possible configurations of the cluster. We get the self-consistent CCPA equations from the condition that the configuration-averaged Green's function obtained by this technique is equal to the Green's function of the effective medium. Depending upon the size of the cluster we can generate various kinds of effective medium. For example, if we take a one-atom cluster we will get the CPA condition. Thus our formulation offers a convenient and systematic way of going beyond the CPA.

B. The KKR-CCPA

In this section we discuss the application of the augmented-space technique to the KKR Green's-function[1,2,30] method of calculating electronic structure for a system of muffin-tin potentials. The Hamiltonian for such a system can be written (in atomic units) as

$$H = -\nabla^2 + \sum_i v_i(\mathbf{r} - \mathbf{R}_i) \ , \tag{2.10}$$

where v_i are the muffin-tin potentials centered at the position of the sites, $\mathbf{R}_i$. The Green's function for this system is given by[30]

$$\underline{G}(\mathbf{r},\mathbf{r}';E) = \sum_{LL'} \underline{Z}^i_L(\mathbf{r}_i)\underline{T}^{ij}_{LL'}\underline{Z}^j_{L'}(\mathbf{r}'_j) - \delta_{ij}\sum_L \underline{Z}^i_L(\mathbf{r}_i)\underline{J}^i_L(\mathbf{r}'_j) \ , \tag{2.11}$$

where $\mathbf{r}$ and $\mathbf{r}'$ lie on ith and jth cells, respectively. The wave functions $\underline{Z}^i_L(\mathbf{r}_i)$ and $\underline{J}^i_L(\mathbf{r}_i)$ are, respectively, the regular and irregular solutions of the differential equation,[30]

$$[-\nabla^2 + v_i(\mathbf{r}_i) - E]\underline{Z}^i_L(\mathbf{r}_i) = 0 \ , \tag{2.12}$$

and $\underline{T}^{ij}_{LL'}$ are on-the-shell matrix elements of path operators given by

$$\underline{T}^{ij}_{LL'} = (\underline{A}^{-1})^{ij}_{LL'} \ ,$$

where

$$\underline{A}^{ij}_{LL'} = \underline{C}^i_{LL'}\,\delta_{ij} - \underline{B}^{ij}_{LL'} \ , \tag{2.13}$$

and $\underline{C}^i_{LL'}$ is the inverse of the on-the-shell single scatterer t matrix. Suppressing the angular momentum indices we can write

$$\underline{T}^{ij} = [(\underline{C}^i\underline{I} - \underline{B})^{-1}]^{ij} \ , \tag{2.14}$$

where $\underline{B}$ is the matrix with elements $\underline{B}^{ij}$ which depend only on the lattice structure[3] and do not contain any randomness, while $\underline{C}^i$ carry the information about randomness. The nonrandomness of the off-diagonal terms $\underline{B}^{ij}$, in the KKR framework, in contrast to the tight-binding framework, where randomness comes both in the diagonal as well as off-diagonal terms, makes the application of the ASF to the KKR framework theoretically much simpler. The first step towards implementing the ASF to the present problem is to write $\underline{C}^i$ in terms of the random variable n_i, i.e.,

$$\underline{C}^i = \underline{C}^B + \delta\underline{C}n_i \ ,$$

where

$$\delta\underline{C} = \underline{C}^A - \underline{C}^B \ . \tag{2.15}$$

From Eq. (2.13), the matrix $\underline{A}$ can be written as

$$\underline{A} = \sum_i \underline{C}^i|i\rangle\langle i| - \sum_{i,j(i\neq j)} \underline{B}^{ij}|i\rangle\langle j| = \underline{C}^B\sum_i |i\rangle\langle i| + \delta\underline{C}\sum_i |i\rangle\langle i|n_i - \sum_{i,j(i\neq j)} \underline{B}^{ij}|i\rangle\langle j| \ . \tag{2.16}$$

Our aim is to find configuration-averaged $\underline{T}^{ij}$, which by the augmented-space theorem, is given by

$$\langle \underline{T}^{ij} \rangle = \langle i,F|\tilde{\underline{A}}^{-1}|j,F\rangle \ , \tag{2.17}$$

where

$$\tilde{\underline{A}} = \underline{C}^B\sum_i |i\rangle\langle i| \otimes \underline{I} + \delta\underline{C}\sum_i |i\rangle\langle i| \otimes \underline{M}^{(i)} - \sum_{i,j(i\neq j)} \underline{B}^{ij}|i\rangle\langle j| \otimes \underline{I} \ . \tag{2.18}$$

In Eq. (2.18) $\underline{I}$ and $\underline{M}^{(i)}$ are operators in the configuration space Φ. Now we partition the augmented

space ψ into subspaces labeled by I and II; the subspace I is spanned by $\{|i,F_s\rangle\}$, $i\in\mathcal{C}$, where $\mathcal{C}$ is the chosen cluster and $\{|F_s\rangle\}$ span the configuration space of the cluster. For a cluster of size m, the subspace I is of rank $m\times 2^m$. The crucial mean-field approximation now involves replacing the conjugate space II by an effective medium. Thus the subspace II has only one configuration, namely, the ground state $|F\rangle$, and hence, is spanned by $\{|j,F\rangle\}$, $j\in\mathcal{C}'$, where $\mathcal{C}'$ is the complement of the cluster $\mathcal{C}$ and is of rank $N-m$.

Since we need the $\langle i,F|\ldots|j,F\rangle$ element $(i,j\in\mathcal{C})$ of $\underline{\tilde{A}}^{-1}$ in Eq. (2.17), we partition $\underline{\tilde{A}}$ as follows:

$$\underline{\tilde{A}}=\begin{bmatrix}\underline{A}_{\mathrm{I}} & \underline{A}' \\ \underline{A}'^{T} & \underline{A}_{\mathrm{II}}\end{bmatrix}, \tag{2.19}$$

where $\underline{A}_{\mathrm{I}}$ is in the subspace I and $\underline{A}_{\mathrm{II}}$ is in the subspace II. By partition theorem, we get the inverse of $\underline{\tilde{A}}$ in subspace I as

$$[\underline{\tilde{A}}^{-1}]_{\mathrm{I}}=(\underline{A}_{\mathrm{I}}-\underline{A}'\underline{A}_{\mathrm{II}}^{-1}\underline{A}'^{T})^{-1}=\underline{\hat{A}}^{-1}. \tag{2.20}$$

The four constituent matrices of $\underline{\tilde{A}}$ are given by

$$\begin{aligned}\underline{A}_{\mathrm{I}}=&\underline{C}^{B}\sum_{i\in\mathcal{C}}|i\rangle\langle i|\otimes\sum_{F_s\in\Phi}|F_s\rangle\langle F_s| \\ &+\delta\underline{C}\sum_{i\in\mathcal{C}}|i\rangle\langle i|\otimes\underline{M}^{(i)} \\ &-\sum_{\substack{i,j\in\mathcal{C}\\(i\neq j)}}\underline{B}^{ij}|i\rangle\langle j|\otimes\sum_{F_s\in\Phi}|F_s\rangle\langle F_s|,\end{aligned} \tag{2.21}$$

$$\begin{aligned}\underline{A}_{\mathrm{II}}=&\Bigg[\underline{C}_{\mathrm{eff}}\sum_{k\in\mathcal{C}'}|k\rangle\langle k|-\sum_{\substack{k,l\in\mathcal{C}'\\(k\neq l)}}\underline{b}^{kl}|k\rangle\langle l| \\ &-\sum_{\substack{k,l\in\mathcal{C}'\\(k\neq l)}}\underline{B}^{kl}|k\rangle\langle l|\Bigg]\otimes|F\rangle\langle F|,\end{aligned} \tag{2.22}$$

$$\begin{aligned}\underline{A}'=&-\Bigg[\sum_{i\in\mathcal{C}}\sum_{k\in\mathcal{C}'}\underline{b}^{ik}|i\rangle\langle k|+\sum_{i\in\mathcal{C}}\sum_{k\in\mathcal{C}'}\underline{B}^{ik}|i\rangle\langle k|\Bigg] \\ &\otimes\sum_{F_s\in\Phi}|F_s\rangle\langle F|,\end{aligned} \tag{2.23}$$

and $\underline{A}'^{T}$ is the transpose of $\underline{A}'$. In Eqs. (2.22) and (2.23), $\underline{b}^{kl}$ are the off-diagonal corrections in $\underline{C}$, the diagonal corrections already contained in $\underline{C}_{\mathrm{eff}}$. Note that $\underline{A}_{\mathrm{I}}$ does not contain $\underline{b}^{ij}$, because subspace I contains the real atoms and their configurations, while $\underline{A}_{\mathrm{II}}$ has these off-diagonal corrections, because subspace II contains only effective atoms. This partitioning of the augmented space into subspaces I and II is different from the physical partition of the lattice into nonoverlapping clusters of the Tsukada scheme.[8] In the present scheme, the subspaces I and II are interacting and, therefore, the operator $\underline{A}'$, which connects the subspaces I and II, must contain the off-diagonal corrections $\underline{b}^{ik}$, in order to include correlated scattering between a site inside the cluster and site outside the cluster.[21] This ensures that the CCPA preserves the translational invariance of the effective medium. Removing $\underline{b}^{ik}$ from $\underline{A}'$ in Eq. (2.23) will lead to the old Tsukada scheme,[8] which is not the same as our CCPA. In general, $\underline{b}^{kl}$ will not be zero in KKR-CCPA. However, for a one-atom cluster, these terms vanish, thus reducing to the correct KKR-CPA limit. For convenience, we add $\underline{b}^{kl}$ to $\underline{B}^{kl}$ (which are also off-diagonal in site indices) and define $\underline{B}^{kl}_{\mathrm{eff}}$ as

$$\underline{B}^{kl}_{\mathrm{eff}}=\underline{B}^{kl}+\underline{b}^{kl}. \tag{2.24}$$

Thus Eqs. (2.22) and (2.23) can now be written as

$$\begin{aligned}\underline{A}_{\mathrm{II}}=&\Bigg[\underline{C}_{\mathrm{eff}}\sum_{k\in\mathcal{C}'}|k\rangle\langle k|-\sum_{\substack{k,l\in\mathcal{C}'\\(k\neq l)}}\underline{B}^{kl}_{\mathrm{eff}}|k\rangle\langle l|\Bigg] \\ &\otimes|F\rangle\langle F|\end{aligned} \tag{2.25}$$

and

$$\underline{A}'=-\Bigg[\sum_{i\in\mathcal{C}}\sum_{k\in\mathcal{C}'}\underline{B}^{ik}_{\mathrm{eff}}|i\rangle\langle k|\Bigg]\otimes\sum_{F_s\in\Phi}|F_s\rangle\langle F|. \tag{2.26}$$

The elements of $\underline{\hat{A}}$ in Eq. (2.20) can be found if we can evaluate the triple product $(\underline{A}'\underline{A}_{\mathrm{II}}^{-1}\underline{A}'^{T})$. Since $\underline{A}_{\mathrm{II}}$ is the matrix in the effective medium with the cluster $\mathcal{C}$ removed, we have

$$\underline{A}_{\mathrm{II}}^{-1}=\underline{T}^{(\mathcal{C})}_{\mathrm{eff}}. \tag{2.27}$$

The superscript $\mathcal{C}$ inside the parentheses indicates that $\underline{T}^{(\mathcal{C})}_{\mathrm{eff}}$ is the path operator matrix of the effective medium with the cluster removed from the medium. Though it is not possible to calculate this quantity, we show in Appendix A that it can be eliminated completely from the computational procedure. From Eqs. (2.25), (2.26), and (2.27) we get

$$\begin{aligned}\underline{A}'\underline{A}_{\mathrm{II}}^{-1}\underline{A}'^{T}=&\sum_{i,j\in\mathcal{C}}\sum_{k,l\in\mathcal{C}'}\underline{B}^{ik}_{\mathrm{eff}}\underline{T}^{(\mathcal{C})kl}_{\mathrm{eff}}\underline{B}^{lj}_{\mathrm{eff}}|i\rangle\langle j| \\ &\otimes\sum_{F_s\in\Phi}|F_s\rangle\langle F_s| \\ =&\sum_{i,j\in\mathcal{C}}\underline{\xi}^{ij}_{\mathcal{C}}|i\rangle\langle j|\otimes\sum_{F_s\in\Phi}|F_s\rangle\langle F_s|,\end{aligned}$$

where

$$\underline{\xi}^{ij}_{\mathcal{C}}=\sum_{k,l\in\mathcal{C}'}\underline{B}^{ik}_{\mathrm{eff}}\underline{T}^{(\mathcal{C})kl}_{\mathrm{eff}}\underline{B}^{lj}_{\mathrm{eff}}\quad\text{for } i,j\in\mathcal{C}. \tag{2.28}$$

It is clear from Eq. (2.28) that the matrix $(\underline{A}'\underline{A}_{\mathrm{II}}^{-1}\underline{A}'^{T})$ is diagonal in the configuration space Φ. The off-diagonal parts in $\underline{\hat{A}}$ thus come from $\underline{A}_{\mathrm{I}}$ only. From Eqs. (2.20), (2.21), and (2.28) we get

$$\begin{aligned}\underline{\hat{A}}=&\Bigg[\sum_{i\in\mathcal{C}}(\underline{C}^{B}-\underline{\xi}^{ii}_{\mathcal{C}})|i\rangle\langle i|-\sum_{\substack{i,j\in\mathcal{C}\\(i\neq j)}}(\underline{B}^{ij}+\underline{\xi}^{ij}_{\mathcal{C}})|i\rangle\langle j|\Bigg] \\ &\otimes\sum_{F_s\in\Phi}|F_s\rangle\langle F_s|+\delta\underline{C}\sum_{i\in\mathcal{C}}|i\rangle\langle i|\otimes\underline{M}^{(i)}.\end{aligned} \tag{2.29}$$

We now partition $\underline{\hat{A}}$ as follows:

$$\underline{\hat{A}}=\begin{bmatrix}\underline{A}_1 & \underline{A}_{12} \\ \underline{A}_{21} & \underline{A}_2\end{bmatrix}, \tag{2.30}$$

where $\underline{A}_1$ is in the subspace 1 spanned by $|i,F\rangle$, $i\in\mathcal{C}$ and is of rank m. The subspace 2 is the complement of

subspace 1 and has rank $m\times(2^m-1)$. The inverse of $\hat{\underline{A}}$ in subspace 1 is then given by

$$[\hat{\underline{A}}^{-1}]_1=(\underline{A}_1-\underline{A}_{12}\underline{A}_2^{-1}\underline{A}_{21})^{-1}\ . \tag{2.31}$$

Since the ranks of the matrices $\underline{A}_1$, $\underline{A}_{12}$, $\underline{A}_{21}$, and $\underline{A}_2$ are small, it is not difficult to find the matrix elements in Eq. (2.31). In Appendix A we show that these can be found analytically for small clusters.

The matrix $\underline{A}_1$ can be obtained from Eq. (2.29) as

$$\underline{A}_1=\sum_{i\in\mathcal{C}}(\bar{\underline{C}}-\underline{\xi}_{\mathcal{C}}^{ii})|i\rangle\langle i|-\sum_{\substack{i,j\in\mathcal{C}\\(i\neq j)}}(\underline{B}^{ij}+\underline{\xi}_{\mathcal{C}}^{ij})|i\rangle\langle j|\ , \tag{2.32}$$

where

$$\bar{\underline{C}}=x\underline{C}^A+y\underline{C}^B\ .$$

From Eq. (2.17) we get

$$\langle\underline{T}^{ij}\rangle=\langle i|(\underline{A}_1-\underline{A}_{12}\underline{A}_2^{-1}\underline{A}_{21})^{-1}|j\rangle\quad\text{for } i,j\in\mathcal{C}\ . \tag{2.33}$$

For the translationally invariant effective medium, Eq. 2.16) can be rewritten as

$$\underline{A}_{\rm eff}=\underline{C}_{\rm eff}\sum_i|i\rangle\langle i|-\sum_{\substack{i,j\\(i\neq j)}}\underline{B}_{\rm eff}^{ij}|i\rangle\langle j|\ . \tag{2.34}$$

We get the effective path operators, for the sites inside he cluster, from Eq. (2.34) by the partitioning technique is

$$\underline{T}_{\rm eff}^{ij}=\left\langle i\left|\left[\sum_{k\in\mathcal{C}}(\underline{C}_{\rm eff}-\underline{\xi}_{\mathcal{C}}^{kk})|k\rangle\langle k|-\sum_{\substack{k,l\in\mathcal{C}\\(k\neq l)}}(\underline{B}_{\rm eff}^{kl}+\underline{\xi}_{\mathcal{C}}^{kl})|k\rangle\langle l|\right]^{-1}\right|j\right\rangle\ . \tag{2.35}$$

The self-consistency condition $\langle\underline{T}^{ij}\rangle=\underline{T}_{\rm eff}^{ij}$ implies that

$$\underline{A}_1-\underline{A}_{12}\underline{A}_2^{-1}\underline{A}_{21}=\sum_{i\in\mathcal{C}}(\underline{C}_{\rm eff}-\underline{\xi}_{\mathcal{C}}^{ii})|i\rangle\langle i|-\sum_{\substack{i,j\in\mathcal{C}\\(i\neq j)}}(\underline{B}_{\rm eff}^{ij}+\underline{\xi}_{\mathcal{C}}^{ij})|i\rangle\langle j|\ . \tag{2.36}$$

The KKR-CCPA equations follow directly from Eq. (2.36) as

$$\underline{C}_{\rm eff}=\bar{\underline{C}}-\langle i|\underline{A}_{12}\underline{A}_2^{-1}\underline{A}_{21}|i\rangle\ , \tag{2.37a}$$

$$\underline{b}^{ij}=\langle i|\underline{A}_{12}\underline{A}_2^{-1}\underline{A}_{21}|j\rangle\quad\text{for } ij(i\neq j)\in\mathcal{C}\ . \tag{2.37b}$$

The path operator matrices can be calculated by the usual k-space integration over the first Brillouin zone as

$$\underline{T}_{\rm eff}^{nm}=\frac{\Omega}{8\pi^3}\int_{\rm BZ}[\underline{C}_{\rm eff}-\underline{B}_{\rm eff}(\mathbf{k},E)]^{-1}\exp(-i\mathbf{k}\cdot\mathbf{R}_{nm})d\mathbf{k}\ , \tag{2.38}$$

where $\underline{B}_{\rm eff}(\mathbf{k},E)$ is the Fourier transform of $\underline{B}_{\rm eff}^{nm}$, i.e.,

$$\underline{B}_{\rm eff}(\mathbf{k},E)=\sum_n\underline{B}_{\rm eff}^{0n}\exp(i\mathbf{k}\cdot\mathbf{R}_{0n})=\underline{B}(\mathbf{k},E)+\sum_{i\in\mathcal{C}}\underline{b}^{0i}\exp(i\mathbf{k}\cdot\mathbf{R}_{0i})\ . \tag{2.39}$$

Note that

$$\underline{b}^{ji}=(\underline{b}^{ij})^T\ ,$$

and therefore we need to solve Eq. (2.37b) for $j>i$ only. This reduces the number of self-consistent coupled equations in Eqs. (2.37a) and (2.37b) to $m(m-1)/2+1$. This number can be further reduced by exploiting the symmetry of the cluster. Note that all these equations involve matrices of rank $(l+1)^2$, where l is the maximum number of angular momentum states used in evaluating the phase shifts. Therefore, with modern computing facilities, solving KKR-CCPA equations for a five-site cluster (for which there are 11 coupled equations) will not be difficult at all.

A cluster consisting of a central site and its shell of nearest neighbors should be the ideal choice but it will be computationally demanding and so we propose an alternative, though approximate method. One can take a two-atom cluster consisting of the central site (site 0) and one of its nearest neighbors (say, site 1). The KKR-CCPA equations for a two-atom cluster are given in Appendix A. By solving equations, one can obtain $\underline{C}_{\rm eff}$ and $\underline{b}^{01}$. Then $\underline{b}^{0m}$, for the rest of the nearest neighbors, can be found by rotational symmetry, since $\underline{b}^{ij}$ will transform like $\underline{B}^{ij}$. These $\underline{b}^{0i}$ can then be used in Eq. (2.39).

C. The configuration-averaged Green's function

The configuration-averaged Green's functions for site-diagonal (SD) and non-site-diagonal (NSD) cases can be written from Eq. (2.11) as

$$\langle\underline{G}_{\rm SD}(\mathbf{r},\mathbf{r}';E)\rangle=\mathrm{Tr}\langle\underline{F}^{ii}(\mathbf{r}_i,\mathbf{r}_i')\underline{T}^{ii}\rangle-\sum_L\langle\underline{Z}_L^i(\mathbf{r}_i)\underline{J}_L^i(\mathbf{r}_i')\rangle$$

and

$$\langle\underline{G}_{\rm NSD}(\mathbf{r},\mathbf{r}';E)\rangle=\mathrm{Tr}\langle\underline{F}^{ij}(\mathbf{r}_i,\mathbf{r}_j')\underline{T}^{ij}\rangle\ , \tag{2.40}$$

where the trace is over the angular momentum indices only and

$$\underline{F}_{LL'}^{ii}(\mathbf{r}_i,\mathbf{r}_i')=\underline{Z}_L^i(\mathbf{r}_i)\underline{Z}_{L'}^i(\mathbf{r}_i')\ ,$$
$$\underline{F}_{LL'}^{ij}(\mathbf{r}_i,\mathbf{r}_j')=\underline{Z}_L^i(\mathbf{r}_i')\underline{Z}_{L'}^j(\mathbf{r}_i)\ . \tag{2.41}$$

To find the joint averages in Eq. (2.40) we adopt the method of Ref. 30. In this method, a single atom is treated exactly, while the rest is effective medium. Equation (2.40) can now be written as

$$\langle \underline{G}_{SD}(\mathbf{r},\mathbf{r}';E)\rangle = \mathrm{Tr}[x\underline{F}^{A}(\mathbf{r}_i,\mathbf{r}_i')\langle \underline{T}^{ii}\rangle_A + y\underline{F}^{B}(\mathbf{r}_i,\mathbf{r}_i')\langle \underline{T}^{ii}\rangle_B] - \sum_L [x\underline{Z}_L^{A}(\mathbf{r}_i)\underline{J}_L^{A}(\mathbf{r}_i') + y\underline{Z}_L^{B}(\mathbf{r}_i)\underline{J}_L^{B}(\mathbf{r}_i')]$$

and

$$\langle \underline{G}_{NSD}(\mathbf{r},\mathbf{r}';E)\rangle = \mathrm{Tr}[x^2\underline{F}^{AA}(\mathbf{r}_i,\mathbf{r}_j')\langle \underline{T}^{ij}\rangle_{AA} + y^2\underline{F}^{BB}(\mathbf{r}_i,\mathbf{r}_j')\langle \underline{T}^{ij}\rangle_{BB} + xy[\underline{F}^{AB}(\mathbf{r}_i,\mathbf{r}_j')\langle \underline{T}^{ij}\rangle_{AB} + \underline{F}^{BA}(\mathbf{r}_i,\mathbf{r}_j')\langle \underline{T}^{ij}\rangle_{BA}]] , \tag{2.42}$$

where $\langle \underline{T}^{ii}\rangle_\alpha$ and $\langle \underline{T}^{ij}\rangle_{\alpha\beta}$ ($\alpha,\beta = A$ or B) are the restricted averages. To find these restricted averages, we embed a single impurity in the effective medium. Now we recall that, in the determination of the effective medium, the off-diagonal term between real and effective atoms is taken as $\underline{B}^{ij}_{\mathrm{eff}}$. Therefore, to be consistent in the prescription of these off-diagonal terms, in the present case also, we take them to be $\underline{B}^{ij}_{\mathrm{eff}}$. In Appendix C, we discuss the effect of change in the off-diagonal terms between real and effective atoms on the DOS. In the present prescription, the restricted averages can be found by a simple partitioning technique, similar to Ref. 30, to give

$$\langle \underline{T}^{ii}\rangle_\alpha = \underline{D}^{\alpha}\underline{T}^{ii}_{\mathrm{eff}} \tag{2.43a}$$

and

$$\langle \underline{T}^{ij}\rangle_{\alpha\beta} = \underline{D}^{\alpha}\underline{T}^{ij}_{\mathrm{eff}}[\underline{I} - (\underline{C}^{\beta} - \underline{C}_{\mathrm{eff}})\underline{D}^{\beta}\underline{T}^{ji}_{\mathrm{eff}}(\underline{C}^{\alpha} - \underline{C}_{\mathrm{eff}}) \times \underline{D}^{\alpha}\underline{T}^{ij}_{\mathrm{eff}}]^{-1}\underline{D}^{\beta} , \tag{2.43b}$$

where

$$\underline{D}^{\alpha} = [\underline{I} + (\underline{C}^{\alpha} - \underline{C}_{\mathrm{eff}})\underline{T}^{00}_{\mathrm{eff}}]^{-1} . \tag{2.44}$$

The total and component DOS's per atom are obtained by integrating the SD Green's function over the unit cell,

$$n(E) = -\frac{1}{\pi}\mathrm{Tr}\,\mathrm{Im}(x\underline{F}^{A}\underline{D}^{A} + y\underline{F}^{B}\underline{D}^{B})\underline{T}^{00}_{\mathrm{eff}} , \tag{2.45}$$

$$n^{\alpha}(E) = -\frac{1}{\pi}\mathrm{Tr}\,\mathrm{Im}\underline{F}^{\alpha}\underline{D}^{\alpha}\underline{T}^{00}_{\mathrm{eff}} , \tag{2.46}$$

where

$$\underline{F}^{\alpha} = \int_{\Omega}\underline{F}^{\alpha}(\mathbf{r}_n,\mathbf{r}_n)d\mathbf{r}_n . \tag{2.47}$$

For the charge self-consistency within the local-density approximation of the density-functional theory, one needs the component charge densities. To find the component charge densities we embed a single atom in the effective medium.[35] The average charge density $\rho(\mathbf{r})$ and component charge density $\rho^{(\alpha)}(\mathbf{r})$ ($\alpha = A,B$) are given by

$$\rho(\mathbf{r}) = -\frac{1}{\pi}\mathrm{Tr}\,\mathrm{Im}\int_{-\infty}^{E_F}[x\underline{F}^{A}(\mathbf{r},\mathbf{r})\underline{D}^{A} + y\underline{F}^{B}(\mathbf{r},\mathbf{r})\underline{D}^{B}] \times \underline{T}^{00}_{\mathrm{eff}}dE , \tag{2.48}$$

$$\rho^{(\alpha)}(\mathbf{r}) = -\frac{1}{\pi}\mathrm{Tr}\,\mathrm{Im}\int_{-\infty}^{E_F}\underline{F}^{\alpha}(\mathbf{r},\mathbf{r})\underline{D}^{\alpha}\underline{T}^{00}_{\mathrm{eff}}dE . \tag{2.49}$$

One can construct the potentials $v^{(\alpha)}(\mathbf{r})$ from $\rho^{(\alpha)}(\mathbf{r})$ in the local-density approximation and thus can achieve charge self-consistency.

For a single impurity of type α in the effective medium, the local DOS on the impurity site can be obtained from Eq. (2.46). If we embed two impurities of type α and β on the sites i and j, respectively, the local DOS on the respective sites will be given by

$$n_2^{(\alpha)}(E) = -\frac{1}{\pi}\mathrm{Tr}\,\mathrm{Im}[\underline{F}^{\alpha}\langle \underline{T}^{ij}\rangle_{ij}]$$

and

$$n_2^{(\beta)}(E) = -\frac{1}{\pi}\mathrm{Tr}\,\mathrm{Im}[\underline{F}^{\beta}\langle \underline{T}^{ji}\rangle_{ij}] . \tag{2.50}$$

Hence we need only to find the path operator matrices $\langle \underline{T}^{ii}\rangle_{ij}$ and $\langle \underline{T}^{ji}\rangle_{ij}$. It is straightforward to obtain these matrices by the partitioning technique. The real space is divided into two subspaces; one for the impurity sites and the other for the rest effective medium. Then by simple matrix algebra one easily gets

$$\langle \underline{T}^{ii}\rangle_{ij} = \{[\underline{T}^{00}_{\mathrm{eff}} - \underline{T}^{ij}_{\mathrm{eff}}(\underline{C}^{\beta} - \underline{C}_{\mathrm{eff}})\underline{D}^{\beta}\underline{T}^{ji}_{\mathrm{eff}}]^{-1} + (\underline{C}^{\alpha} - \underline{C}_{\mathrm{eff}})\}^{-1}$$

and

$$\langle \underline{T}^{jj}\rangle_{ij} = \{[\underline{T}^{00}_{\mathrm{eff}} - \underline{T}^{ji}_{\mathrm{eff}}(\underline{C}^{\alpha} - \underline{C}_{\mathrm{eff}})\underline{D}^{\alpha}\underline{T}^{ij}_{\mathrm{eff}}]^{-1} + (\underline{C}^{\beta} - \underline{C}_{\mathrm{eff}})\}^{-1} . \tag{2.51}$$

Equations (2.46)–(2.51) are rather general and can be used to calculate local DOS and charge densities for a single impurity or two impurities of foreign kind in the effective medium.

III. RESULTS AND DISCUSSION

In this section we present the results of our calculations of DOS for a one-dimensional muffin-tin alloy. All the relevant equations for this model are given in Appendix B. The lattice parameters ($a = 6.00$ a.u.) and the muffin-tin radii ($r_m = 2.25$ a.u.) of the two components of the alloy are identical. The depths of the two constituent potentials are $V_A = -0.3$ Ry and $V_B = -0.5$ Ry. The DOS for the two pure systems is shown in Fig. 1, which shows peaks at band edges, characteristics of the one-dimensional model. For the KKR-CCPA calculations we have taken a two-atom cluster. In Fig. 2 we show the results of our calculations in the low concentration ($x = 0.1$) limit. Figure 2(a) shows the KKR-CPA and KKR-CCPA DOS's. We note that, in the first majority band, there is no apparent difference in the KKR-CPA and KKR-CCPA results. However, in the impurity band we observe a shoulder in the KKR-CCPA DOS around $E \approx -0.16$ Ry and a peak at $E \approx -0.12$ Ry, in contrast to a smooth KKR-CPA impurity band centered around $E = -0.14$ Ry. The extra structures in the KKR-CCPA

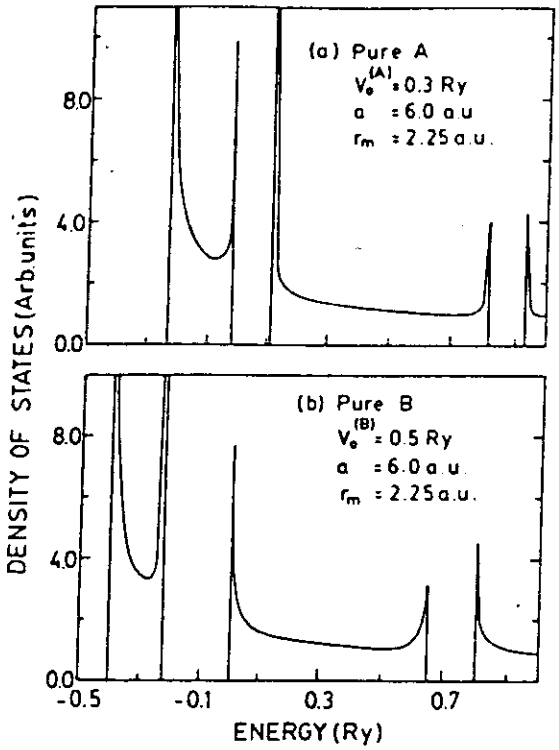

FIG. 1. DOS for the one-dimensional systems of potential depths (a) $V_A = 0.3$ Ry and (b) $V_B = 0.5$ Ry.

DOS seem to arise due to correlated scattering from two-atom clusters. This becomes clear by a close inspection of the local DOS on impurities for a two-impurity cluster embedded in the KKR-CPA medium, as shown in Figs. (2b) and (2c). If we look at the local DOS on the A-type impurity of an AA-type cluster, as shown in Fig. 2(b), we observe that its impurity band is almost identical to that of the KKR-CCPA DOS, thus explaining the above-mentioned structure. We also observe a peak at $E = -0.13$ Ry in the local DOS on the A-type impurity of an AB-type cluster, as shown in Fig. 2(c), which is close to the peak at $E = -0.12$ Ry in the KKR-CCPA DOS. Also, a small but observable structure at $E = 0.06$ Ry in the KKR-CCPA DOS is very close to the two kinks around $E = 0.04$ Ry in the local DOS on both A-type and B-type impurities of an AB-type cluster, as shown in Fig. 2(c). In Fig. 2(d) we show the local DOS on A-type impurities in a pure B medium. We observe that the two-impurity levels at $E = -0.19$ and -0.10 Ry are close enough to the structures in the minority band of the KKR-CCPA DOS. This further supports our assertion that these structures arise from two-impurity scattering.

Figure 3 shows the results for a concentrated alloy ($x = 0.5$). As shown in Fig. 3(a), the KKR-CPA gives a rather smooth DOS besides a peak in each band while the KKR-CCPA, once again gives few extra structures in all the bands. The KKR-CPA peaks at $E = -0.38$, -0.21, and 0.04 Ry almost coincide with the major KKR-CCPA peaks at $E = -0.39$, -0.21, and 0.04 Ry. Besides these major peaks, we observe some more peaks at $E = -0.35$,

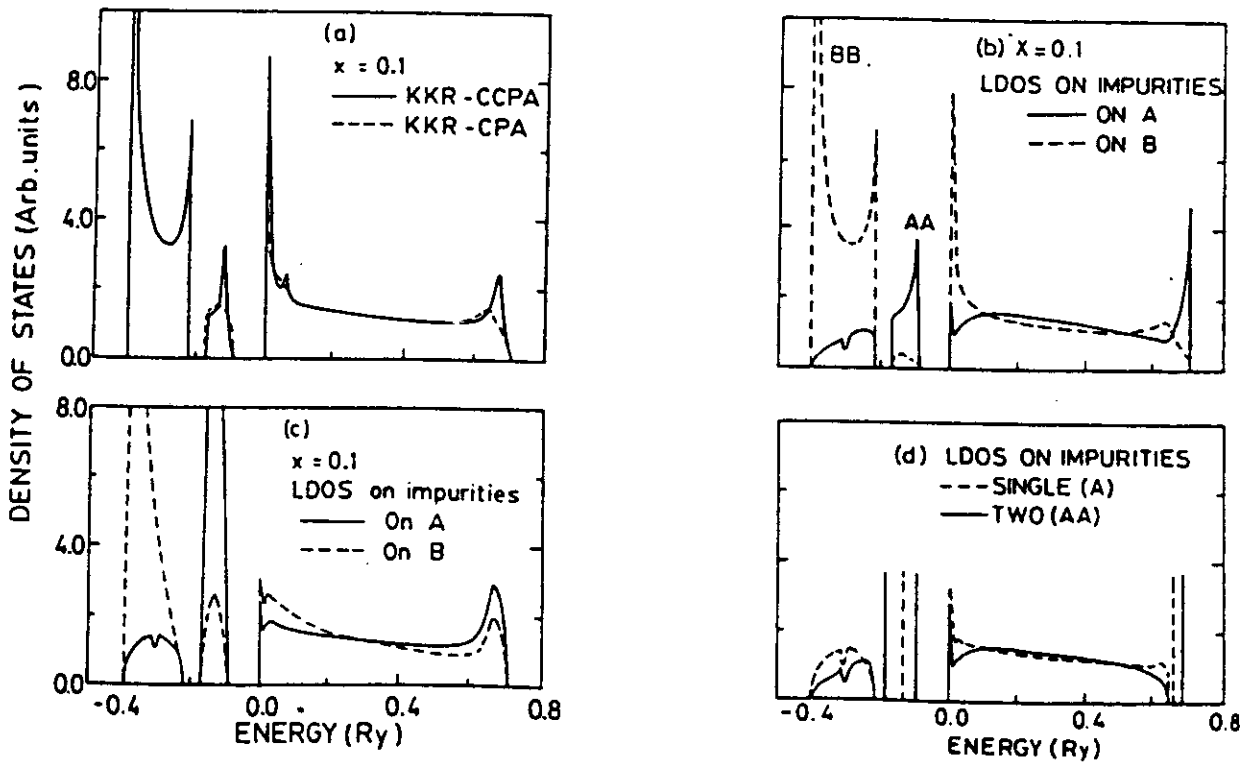

FIG. 2. (a) KKR-CPA (dashed line) and KKR-CCPA (solid line) DOS's for the alloy with concentration $x = 0.1$. (b) Local DOS on the impurity site for a cluster of two impurities of AA (solid line) and BB (dashed line) type embedded in the KKR-CPA medium for $x = 0.1$. (c) Local DOS on the impurity site of A (solid line) and B (dashed line) type of an AB-type cluster embedded in the KKR-CPA medium for $x = 0.1$. (d) Local DOS on the impurity site for a single (dashed line) and two (solid line) impurities of type A embedded in the pure B medium.

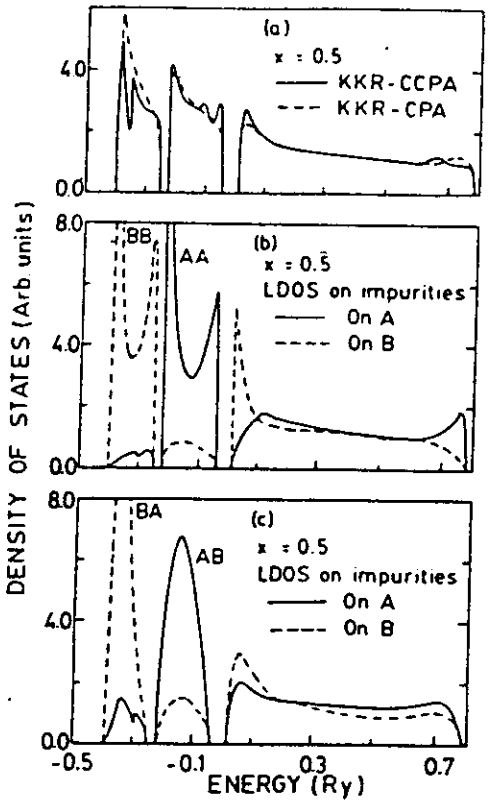

FIG. 3. (a) KKR-CPA (dashed line) and KKR-CCPA (solid line) DOS's for the alloy with concentration $x=0.5$. (b) Local DOS on the impurity site for a cluster of two impurities of AA (solid line) and BB (dashed line) type embedded in the KKR-CPA medium for $x=0.5$. (c) Local DOS on the impurity site of A (solid line) and B (dashed line) type of a cluster of AB type embedded in the KKR-CPA medium for $x=0.5$.

-0.11, and -0.06 Ry, in the KKR-CCPA DOS. As in the case of $x=0.1$, these extra structures in the KKR-CCPA DOS are very close to the structures in the local DOS on the impurities of a two-impurity cluster embedded in the KKR-CPA medium. In Figs. 3(b) and 3(c) we show, respectively, the local DOS's on the impurities of a cluster of two like and unlike impurities embedded in the KKR-CPA medium. We observe that the KKR-CCPA peak at $E=-0.35$ Ry is exactly at the position of the peak in the local DOS on a B-type impurity of an AB-type cluster, as shown in Fig. 3(c). Thus the KKR-CCPA peak at $E=-0.35$ Ry is identified as due to the B-type atoms. The second extra peak at $E=-0.11$ Ry is close to the peak in the local DOS on an A-type impurity of an AB-type cluster, which is at $E=-0.14$ Ry. The third extra peak at $E=-0.06$ Ry can be identified as due to the A-type atoms as it is very close to a peak in the local DOS on an A-type impurity of an AA-type cluster at $E=-0.05$ Ry as shown in Fig. 3(b).

We have also compared our KKR-CCPA results with some calculations obtained by using the embedded cluster approach of Gonis *et al.*[13] We have embedded clusters of two, three, and five atoms in the KKR-CPA medium. The averaged DOS on the central site of the cluster is obtained by calculating the local DOS on the central site for all possible configurations of the clusterand then taking the average. This averaged DOS produces some of the

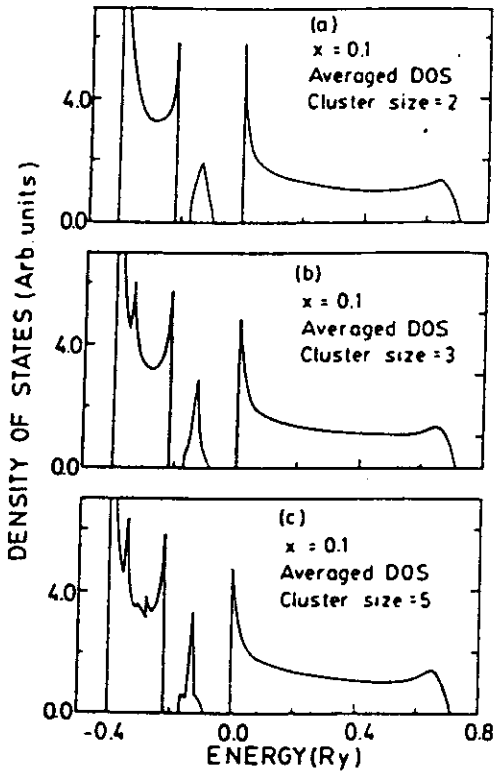

FIG. 4. Averaged DOS on the central site of a cluster of (a) two atoms, (b) three atoms, and (c) five atoms, embedded in the KKR-CPA medium for $x=0.1$.

structures of the KKR-CCPA DOS. In Figs. 4(a), 4(b), and 4(c), we show the averaged DOS, for different cluster size, in the low concentration limit ($x=0.1$). We observe that, for a two-atom cluster, the averaged DOS does not give the structures of the KKR-CCPA DOS.

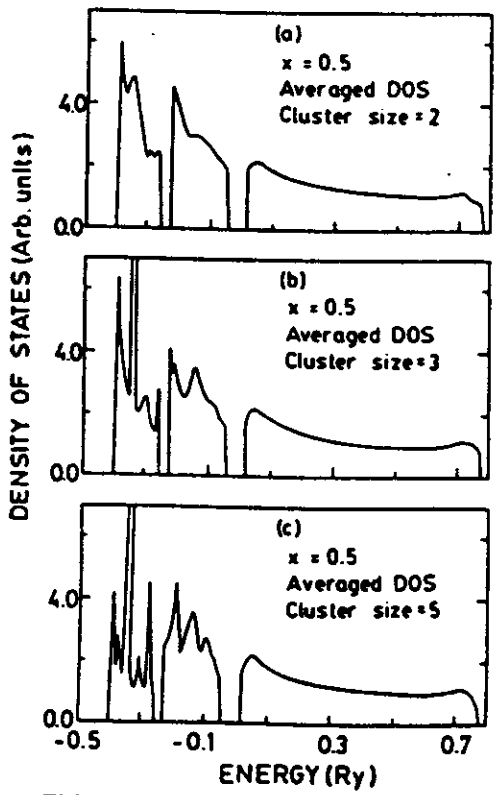

FIG. 5. Same as Fig. 4 except $x=0.5$.

However, as we increase the cluster size, the structures in the averaged DOS become prominent, and show resemblance to the KKR-CCPA results. For the higher concentration ($x=0.5$) also, the averaged DOS, as shown in Figs. 5(a), 5(b), and 5(c), does reproduce the structures of the KKR-CCPA DOS in Fig. 3(a), which become more prominent with the increase in the cluster size.

IV. CONCLUSION

We have shown that one can go beyond the CPA in the first-principles KKR Green's-function method by effectively combining the ASF with the conventional KKR method. It has been put on the same rigorous footing as KKR-CPA in which one can calculate DOS, component DOS, and charge densities, self-consistently. We have shown that the KKR-CCPA, unlike the KKR-CPA, introduces off-diagonal corrections to the scattering matrices. Our calculations on a model alloy show that the structures in the KKR-CCPA DOS are due to correlated scattering from clusters of atoms in the effective medium.

ACKNOWLEDGMENTS

One of the authors (R.P.) thanks Professor V. Heine for his kind hospitality at the Cavendish Laboratory, U.K., and some helpful discussions. He also acknowledges discussions with Professor A. Bansil, Professor R. Haydock, Professor B. L. Gyorffy, and Dr. R. Benedek. This work was supported by the Department of Science and Technology, New Delhi, India, through Grant No. SP/S2/M-39/87.

APPENDIX A: KKR-CCPA FOR ONE- AND TWO-ATOM CLUSTERS

For a one-atom cluster (the 0th site) the configuration space ϕ_0 is spanned by $|f_0^{(0)}\rangle$ and $|f_1^{(0)}\rangle$. Then Eq. (2.21) reduces to

$$\underline{\Delta}_1=\begin{bmatrix}\bar{\underline{C}} & \underline{\omega}\\ \underline{\omega} & \bar{\underline{C}}\end{bmatrix}, \tag{A1}$$

where

$$\bar{\underline{C}}=y\underline{C}^{A}+x\underline{C}^{B}$$

and

$$\underline{\omega}=(xy)^{1/2}(\underline{C}^{A}-\underline{C}^{B}). \tag{A2}$$

Rewriting Eqs. (2.28) and (2.29) for this case we get

$$\underline{\xi}_1^{00}=\sum_{j,k\neq 0}\underline{B}_{\rm eff}^{0j}\underline{T}_{\rm eff}^{(0)jk}\underline{B}_{\rm eff}^{k0} \tag{A3}$$

and

$$\hat{\underline{\Delta}}=\begin{bmatrix}\bar{\underline{C}}-\underline{\xi}_1^{00} & \underline{\omega}\\ \underline{\omega} & \bar{\underline{C}}-\underline{\xi}_1^{00}\end{bmatrix}. \tag{A4}$$

The matrices $\underline{\Delta}_1$ and $\hat{\underline{\Delta}}$ are in a space spanned by $|f_0^{(0)}\rangle$ and $|0,f_1^{(0)}\rangle$. Now for the effective medium we have

$$\underline{T}_{\rm eff}^{00}=\left[\underline{C}_{\rm eff}-\sum_{j,k\neq 0}\underline{B}_{\rm eff}^{0j}\underline{T}_{\rm eff}^{(0)jk}\underline{B}_{\rm eff}^{k0}\right]^{-1}$$
$$=(\underline{C}_{\rm eff}-\underline{\xi}_1^{00})^{-1} \tag{A5}$$

and thus

$$\underline{\xi}_1^{00}=\underline{C}_{\rm eff}-(\underline{T}_{\rm eff}^{00})^{-1}. \tag{A6}$$

By the augmented-space theorem we have

$$\underline{T}_{\rm eff}^{00}=\langle 0,f_0^{(0)}|\hat{\underline{\Delta}}^{-1}|0,f_0^{(0)}\rangle$$
$$=[\bar{\underline{C}}-\underline{\xi}_1^{00}-\underline{\omega}(\bar{\underline{C}}-\underline{\xi}_1^{00})^{-1}\underline{\omega}]^{-1}. \tag{A7}$$

Comparing (A5) and (A7) we get the KKR-CPA equation

$$\underline{C}_{\rm eff}=\bar{\underline{C}}-\underline{\omega}(\bar{\underline{C}}-\underline{\xi}_1^{00})^{-1}\underline{\omega}$$
$$=\bar{\underline{C}}-\underline{\omega}[\bar{\underline{C}}-\underline{C}_{\rm eff}+(\underline{T}_{\rm eff}^{00})^{-1}]^{-1}\underline{\omega}$$

which readily reduces to the familiar form

$$\underline{C}_{\rm eff}=\bar{\underline{C}}+(\underline{C}^{A}-\underline{C}_{\rm eff})\underline{T}_{\rm eff}^{00}(\underline{C}^{B}-\underline{C}_{\rm eff}). \tag{A8}$$

For a two-atom cluster of sites 0 and 1, the configuration space is spanned by four vectors, which are $|F\rangle=|f_0^{(0)}f_0^{(1)}\rangle$, $|F_1\rangle=|f_0^{(0)}f_1^{(1)}\rangle$, $|F_0\rangle=|f_1^{(0)}f_0^{(1)}\rangle$, and $|F_{01}\rangle=|f_1^{(0)}f_1^{(1)}\rangle$. The augmented space is spanned by eight bases $|i,\mathcal{F}\rangle$, $i=0,1$ and $\mathcal{F}=F$, F_0, F_1, and F_{01}.

For this case, Eq. (2.28) reduces to

$$\underline{\xi}_2^{ij}=\sum_{k,l\neq 0,1}\underline{B}_{\rm eff}^{ik}\underline{T}_{\rm eff}^{(0,1)kl}\underline{B}_{\rm eff}^{lj}\quad\text{for } i,j=0,1. \tag{A9}$$

It is evident that $\underline{\xi}_2^{00}=\underline{\xi}_2^{11}$. By partitioning the effective medium to get the path operators for the sites inside the cluster, we get

$$\begin{bmatrix}\underline{T}_{\rm eff}^{00} & \underline{T}_{\rm eff}^{01}\\ \underline{T}_{\rm eff}^{10} & \underline{T}_{\rm eff}^{11}\end{bmatrix}=\left[\begin{bmatrix}\underline{C}_{\rm eff} & -\underline{B}_{\rm eff}^{01}\\ -\underline{B}_{\rm eff}^{10} & \underline{C}_{\rm eff}\end{bmatrix}-\begin{bmatrix}\underline{\xi}_2^{00} & \underline{\xi}_2^{01}\\ \underline{\xi}_2^{10} & \underline{\xi}_2^{11}\end{bmatrix}\right]^{-1},$$

which gives

$$\underline{\xi}_2^{00}=\underline{C}_{\rm eff}-[\underline{T}_{\rm eff}^{00}-\underline{T}_{\rm eff}^{01}(\underline{T}_{\rm eff}^{00})^{-1}\underline{T}_{\rm eff}^{10}]^{-1},$$
$$\underline{\xi}_2^{01}=-\underline{B}_{\rm eff}^{01}+[\underline{T}_{\rm eff}^{00}(\underline{T}_{\rm eff}^{01})^{-1}\underline{T}_{\rm eff}^{00}-\underline{T}_{\rm eff}^{10}]^{-1}, \tag{A10}$$
$$\underline{\xi}_2^{10}=-\underline{B}_{\rm eff}^{10}+[\underline{T}_{\rm eff}^{00}(\underline{T}_{\rm eff}^{10})^{-1}\underline{T}_{\rm eff}^{00}-\underline{T}_{\rm eff}^{01}]^{-1}.$$

Thus with this technique it is possible to eliminate the infinite sum in Eq. (A9) and calculate $\underline{\xi}_2^{ij}$ explicitly in terms of the known effective medium quantities.

Partitioning $\hat{\underline{\Delta}}$ in the scheme of Eq. (2.30) we get

$$\underline{\Delta}_1=\begin{bmatrix}\bar{\underline{C}}-\underline{\xi}_2^{00} & -\underline{V}^{01}\\ -\underline{V}^{10} & \bar{\underline{C}}-\underline{\xi}_2^{00}\end{bmatrix},$$

$$\underline{\Delta}_{12}=\begin{bmatrix}0&0&0&0&0&\omega\\ \omega&0&0&0&0&0\end{bmatrix}, \tag{A11}$$

$$\underline{\Delta}_{21}=\underline{\Delta}_{12}^{T},$$

where

$$\underline{V}^{ij}=\underline{B}^{ij}+\underline{\xi}_2^{ij}\quad\text{for } i,j=0,1. \tag{A12}$$

Now the KKR-CCPA equations (2.37a) and (2.37b)

$$\underline{C}_{\rm eff}=\bar{\underline{C}}-\langle 0|\underline{A}_{12}\underline{A}_{2}^{-1}\underline{A}_{21}|0\rangle=\bar{\underline{C}}-\underline{\omega}\underline{Q}^{00}\underline{\omega}$$

and

$$\underline{b}^{01}=\langle 0|\underline{A}_{12}\underline{A}_{2}^{-1}\underline{A}_{21}|1\rangle=\underline{\omega}\underline{Q}^{01}\underline{\omega}\ , \tag{A13}$$

where

$$\begin{aligned}
&\underline{Q}^{00}=R_6^{-1}\ ,\\
&\underline{Q}^{01}=R_6^{-1}V^{01}R_5^{-1}\omega R_4^{-1}V^{10}R_3^{-1}\omega R_2^{-1}V^{01}R_1^{-1}\ ,
\end{aligned} \tag{A14}$$

and

$$\begin{aligned}
R_1&=\bar{\underline{C}}-\underline{\xi}_2^{00}\ ,\\
R_2&=\bar{\underline{C}}-\underline{\xi}_2^{00}-V^{01}R_1^{-1}V^{10}\ ,\\
R_3&=\bar{\underline{C}}-\underline{\xi}_2^{00}-\underline{\omega}R_2^{-1}\omega\ ,\\
R_4&=\bar{\underline{C}}-\underline{\xi}_2^{00}-V^{10}R_3^{-1}V^{01}\ ,\\
R_5&=\bar{\underline{C}}-\underline{\xi}_2^{00}-\omega R_4^{-1}\omega\ ,\\
R_6&=\bar{\underline{C}}-\underline{\xi}_2^{00}-V^{01}R_5^{-1}V^{10}\ .
\end{aligned} \tag{A15}$$

Note that $\underline{C}_{\rm eff}$ may no longer be diagonal in angular momentum space.

APPENDIX B: ONE-DIMENSIONAL ALLOY MODEL

We consider a one-dimensional alloy of nonoverlapping muffin-tin (MT) potentials described by the Hamiltonian

$$H=-\frac{d^2}{dx^2}+\sum_n v_n(x-na)\ . \tag{B1}$$

In close analogy with the MT model in three dimensions we assume that $v_n(x)$ is symmetric in x and vanishes for $|x|\geq r_m$ (the MT radius), $r_m\leq a/2$ (a is the lattice constant). This one-dimensional model retains many of the features of the three-dimensional MT system.[34] But, in this case, we have only two components of angular momentum ($l=0$ and 1).[34] The SD Green's function for this system is given by

$$\mathrm{Im}\underline{G}(x,x')=\sum_{l,l'}\underline{Z}_l(x)\mathrm{Im}(\underline{T}_{ll'}^{00})\underline{Z}_{l'}(x')\ , \tag{B2}$$

where $\underline{Z}_l(x)$ are the solutions of the Schrödinger equation. The on-the-shell matrix elements of the path operators are given by the integral

$$\underline{T}_{\rm eff}^{ij}=\frac{a}{2\pi}\int_{-\pi/a}^{\pi/a}dk[\underline{C}_{\rm eff}-\underline{B}_{\rm eff}(k,E)]^{-1}\exp[ik(i-j)a]\ , \tag{B3}$$

where $\underline{B}_{\rm eff}(k,E)$ are given by Eq. (2.39) as

$$\underline{B}_{\rm eff}(k,E)=\underline{B}(k,E)+\underline{b}^{01}\exp(ika)\ . \tag{B4}$$

$\underline{B}(k,E)$ are the KKR structure functions in one dimension and have explicit expressions.[34] Equation (B3) can be transformed into a contour integration by putting $z=\exp(ika)$:

$$\underline{T}_{\rm eff}^{ij}=\frac{1}{2\pi i}\oint_C dz\,z^{j-i-1}\frac{g(z)}{\lambda z^4+\delta z^3+\alpha z^2+\beta z+\gamma}\ , \tag{B5}$$

where C is the unit circle centered at $z=0$ and $g(z)$ is a matrix in l space and is given by

$$\begin{aligned}
g_{00}(z)&=[z^2+1-2z\cos(Ka)]\\
&\quad\times(i-K\underline{C}_{11}+K\underline{b}_{11}z)+2z\sin(Ka)\ ,\\
g_{11}(z)&=[z^2+1-2z\cos(Ka)]\\
&\quad\times(i-K\underline{C}_{00}+K\underline{b}_{00}z)+2z\sin(Ka)\ ,\\
g_{01}(z)&=K(\underline{C}_{01}-\underline{b}_{01}z)[z^2+1-2z\cos(Ka)]+z^2-1\ ,\\
g_{10}(z)&=K(\underline{C}_{10}-\underline{b}_{10}z)[z^2+1-2z\cos(Ka)]-z^2+1\ ,
\end{aligned} \tag{B6}$$

and the constants appearing in the denominator of (B5) are

$$\begin{aligned}
\lambda&=E(\underline{b}_{00}\underline{b}_{11}-\underline{b}_{01}\underline{b}_{10})\ ,\\
\delta&=\eta-K(\underline{b}_{01}-\underline{b}_{10})-2\lambda\cos(Ka)\ ,\\
\alpha&=\lambda+\gamma+2K(\underline{C}_{01}-\underline{C}_{10})-2\eta\cos(Ka)\ ,\\
\beta&=2\cos(Ka)[2-\gamma-K(\underline{C}_{01}-\underline{C}_{10})]\\
&\quad+2\sin(Ka)[2i-K(\underline{C}_{00}+\underline{C}_{11})]\\
&\quad+\eta+K(\underline{b}_{01}-\underline{b}_{10})\ ,\\
\gamma&=E(\underline{C}_{00}\underline{C}_{11}-\underline{C}_{01}\underline{C}_{10})\\
&\quad-iK(\underline{C}_{00}+\underline{C}_{11})-K(\underline{C}_{01}-\underline{C}_{10})\ ,\\
\eta&=iK(\underline{b}_{00}+\underline{b}_{11})\\
&\quad-E(\underline{C}_{00}\underline{b}_{11}+\underline{C}_{11}\underline{b}_{00}-\underline{C}_{01}\underline{b}_{10}-\underline{C}_{10}\underline{b}_{01})\ .
\end{aligned} \tag{B7}$$

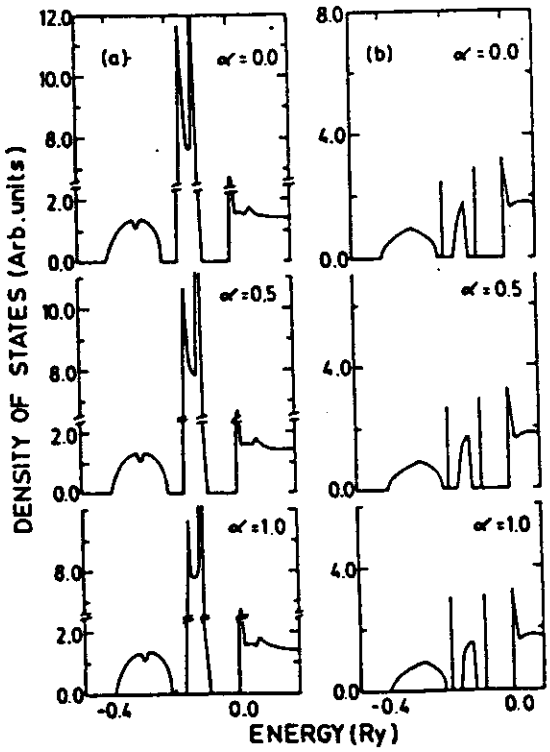

FIG. 6. Local DOS on a single impurity of potential depth (a) 0.3 Ry (type A), and (b) 0.2 Ry, embedded in the KKR-CCPA medium for $x=0.1$, using Eq. (C1). Vertical lines in (b) at -0.2 and -0.1 Ry denote the impurity levels.

In Eqs. (B6) and (B7) $K=\sqrt{E}$ and $\underline{C}\equiv\underline{C}_{\text{eff}}$ and $\underline{b}\equiv\underline{b}^{01}$. Now consider a one-dimensional MT potential,

$$v_n(x)=-V_0^{A(B)}\Theta(r_m-r)\ .$$

The phase shifts are given by

$$\theta_l=-Kr_m+\tan^{-1}\left[\left[\frac{k_l}{K}\right]^{-l}\tan(k_1r_m)\right] \tag{B8}$$

where

$$k_1=(E+V_0)^{1/2}\ .$$

The wave functions $\underline{Z}_l(x)$, both inside and outside the MT cell, can also be found analytically and thus the integral

$$\underline{F}_{ll'}=\int_\Omega \underline{Z}_l(x)\underline{Z}_{l'}(x)dx$$

can be evaluated to give

$$\underline{F}_{ll'}=\frac{\delta_{ll'}}{2E\sin^2\Theta_l}\left[\frac{\cos^2(Kr_m+\Theta_l-l\pi/2)}{\cos^2(k_1r_m-l\pi/2)}\left[r_m+\frac{\sin(2k_1r_m-l\pi)}{2k_1}\right]+\frac{a}{2}-r_m+(-1)^l\left[\frac{\sin(Ka+2\Theta_l)-\sin(2Kr_m+2\Theta_l)}{2K}\right]\right]\ . \tag{B9}$$

The off-diagonal elements of $\underline{F}$ vanish due to opposite parity of the $l=0$ and 1 wave functions.

APPENDIX C: OFF-DIAGONAL TERMS BETWEEN REAL AND EFFECTIVE ATOMS

Let us embed a single atom in the KKR-CCPA medium. We assume the off-diagonal term between real and effective atoms to be of the form

$$\underline{B}^{ij}_{\text{new}}=\underline{B}^{ij}+\alpha(\underline{B}^{ij}_{\text{eff}}-\underline{B}^{ij}),\quad 0\le\alpha\le 1\ . \tag{C1}$$

The case $\alpha=1$, represents the one which we have adopted in Sec. II C. We have calculated local DOS on this impurity embedded in the KKR-CCPA medium using Eq. (C1) for various impurity potentials with different values of α. In Fig. 6(a), we show the local DOS on A-type impurity (potential depth $=0.3$ Ry) for $x=0.1$ and $\alpha=0.0$, 0.5, and 1.0. We observe that there is some variation in the height of the peaks in the local DOS with α, although there is little qualitative change in the DOS. The variation in the height of the peaks for $\alpha=0.0$ and 1.0 is less than 10%. A similar trend is observed in the case of $x=0.5$. Also, for an impurity of foreign kind, the same conclusion can be drawn from Fig. 6(b), which shows local DOS on the impurity of potential depth 0.2 Ry. Although the basic structure of the local DOS does not change with different choices of the off-diagonal terms between real and effective atoms, we feel that further work is needed to clarify the problem of embedding in the KKR-CCPA medium.

*Present address: S. N. Bose National Center for Basic Sciences, DB-17, Sector I Salt Lake, Calcutta 700064, India.

[1]A. Bansil, in *Electronic Band Structure and its Applications*, edited by M. Yussouff (Springer-Verlag, Berlin, 1987), p. 273.
[2]J. S. Faulkner, in *Progress in Materials Science*, edited by J. W. Christian, P. Hassen, and T. Massalski (Pergamon, New York, 1982), Vol. 27, p. 1.
[3]H. Ehrenreich and L. Schwartz, in *Solid State Physics*, edited by H. Ehrenreich, F. Seitz, and D. Turnbull (Academic, New York, 1976), Vol. 31, p. 149.
[4]H. Wright, P. Weightman, P. T. Andrews, W. Folkerts, C. F. J. Flipse, G. A. Sawatzky, D. Norman, and H. Padmore, Phys. Rev. B 35, 519 (1987).
[5]D. van der Marel, J. A. Jullianus, and G. A. Sawatzky, Phys. Rev. B 32, 6331 (1985).
[6]J. Banhart, W. Pfeiler, and J. Voitlander, Phys. Rev. B 37, 6027 (1988).
[7]B. G. Nickel and J. A. Krumhansl, Phys. Rev. B 4, 4354 (1971).
[8]M. Tsukada, J. Phys. Soc. Jpn. 26, 684 (1969); 32, 1475 (1972).
[9]W. H. Butler, Phys. Rev. B 8, 4499 (1973).
[10]N. F. Berk, J. Shazeer, and R. A. Tahir-Kheli, Phys. Rev. B 8, 2496 (1973).
[11]A. Gonis and J. W. Garland, Phys. Rev. B 16, 2424 (1977).
[12]A. Gonis, W. H. Butler, and G. M. Stocks, Phys. Rev. Lett. 50, 1482 (1983).
[13]A. Gonis, G. M. Stocks, W. H. Butler, and H. Winter, Phys. Rev. B 29, 555 (1984).
[14]A. Gonis and A. J. Freeman, Phys. Rev. B 29, 4277 (1984).
[15]B. G. Nickel and W. H. Butler, Phys. Rev. Lett. 30, 373 (1973).
[16]A. R. Bishop and A. Mookerjee, J. Phys. C 7, 2165 (1974).
[17]R. Mills and P. Ratanavararaksa, Phys. Rev. B 18, 5291 (1978).
[18]T. Kaplan, P. L. Leath, L. J. Gray, and H. W. Diehl, Phys. Rev. B 21, 4230 (1980).
[19]P. L. Leath, in *Excitations in Disordered Systems*, edited by M. F. Thorpe (Plenum, New York, 1981), p. 109; T. Kaplan and L. J. Gray, *ibid.*, p. 129.
[20]A. Mookerjee, in *Electronic Band Structure and its Applications*, edited by M. Yussouff (Springer-Verlag, Berlin, 1987), p. 248.
[21]V. Kumar, A. Mookerjee, and V. K. Srivastava, J. Phys. C 15,

1939 (1982); P. K. Thakur, A. Mookerjee, and V. A. Singh, J. Phys. F 17, 1523 (1987).
[22]R. Mills, L. J. Gray, and T. Kaplan, Phys. Rev. B 27, 3252 (1983).
[23]T. Kaplan and L. J. Gray, Phys. Rev. B 29, 3684 (1984).
[24]A. Mookerjee, J. Phys. F 17, 1511 (1987); S. S. Rajput, S. S. A. Razee, R. Prasad, and A. Mookerjee, J. Phys. Condensed Matter 2, 2653 (1990).
[25]N. Stefanou, R. Zeller, and P. H. Dederichs, Solid State Commun. 62, 735 (1987).
[26]A. Mookerjee, J. Phys. C 6, L205 (1973); 6, 1340 (1973).
[27]L. J. Gray and T. Kaplan, Phys. Rev. B 14, 3462 (1976); 15, 6005 (1977); J. Phys. C 9, L303 (1976); 9, L483 (1976).
[28]A. Mookerjee, J. Phys. C 9, 1225 (1976); 19, 193 (1986); 19, 275 (1986).
[29]S. S. A. Razee, A. Mookerjee, and R. Prasad (unpublished).
[30]J. S. Faulkner and G. M. Stocks, Phys. Rev. B 21, 3222 (1980).
[31]A. Gonis and G. M. Stocks, Phys. Rev. B 25, 659 (1982).
[32]P. K. Thakur and A. Mookerjee, Phys. Rev. B 38, 3798 (1988).
[33]L. J. Gray and T. Kaplan, Phys. Rev. B 24, 1872 (1981).
[34]W. H. Butler, Phys. Rev. B 14, 468 (1976).
[35]In principle, one can embed a cluster of impurities to find charge densities for different configurations of the cluster. The component charge density $\rho^{[\alpha]}(\mathbf{r})$ on a particular impurity α will be different for different configurations of impurities around it. This, in turn, will give us different $v^{[\alpha]}(\mathbf{r})$ for different configurations of the cluster. For example, for a two-atom cluster, $v^{[A]}(\mathbf{r})$ will be different for AA- and AB-type clusters. However, in our formulation, we assume $v^{[A]}(\mathbf{r})$ to be the same for AA- and AB-type clusters. Therefore we do not need different $v^{[\alpha]}(\mathbf{r})$ for different clusters.

J. Phys.: Condens. Matter 3 (1991) 801–812. Printed in the UK

Shockley-type surface states on low-index faces of Cu-based alloys with polyvalent solutes

R Prasad†, A Y Serageldin and A Bansil
Department of Physics, Northeastern University, Boston, MA 02115, USA

Received 23 August 1990

Abstract. We consider Shockley-type surface states (SSS) in substitutionally disordered alloys. For this purpose the Green function for the semi-infinite system is obtained by matching the bulk Korringa–Kohn–Rostoker coherent potential approximation (KKR-CPA) Green function with the free-electron Green function on the bounding surface. The formalism is applied to calculate binding energies and disorder induced smearings of the $\bar{Y}$-centred SSS on the (110) surface and the $\bar{\Gamma}$- centred SSS on the (111) surfaces of Cu, $Cu_{90}Al_{10}$, $Cu_{70}Zn_{30}$, and $Cu_{90}Ge_{10}$. Our theoretical predictions with regard to changes in the binding energy and the disorder induced smearing in $Cu_{90}Al_{10}$ where corresponding angle-resolved photoemission experiments are available for comparison are in reasonable accord with measurements. Our computations indicate that the binding energy of the SSS in Cu-based alloys will generally increase with increasing electron/atom (e/a) ratio.

1. Introduction

Although the bulk electronic structure of disordered alloys has been studied extensively in recent years, relatively little work exists concerning their surface electronic structure. As is well known, the presence of the surface can induce substantial changes in electronic structure, causing in particular the appearance of new types of states localized in the surface region; such surface states have in fact been observed in angle-resolved photoemission experiments in a number of alloys (Pessa *et al* 1981, Asonen *et al* 1982, Jordan and Sohal 1982, Rao *et al* 1984, Asonen *et al* 1985, Heimann *et al* 1981; for a review see Bansil and Pessa 1983, Jordan and Durham 1989.) In this article, we consider one class of surface states, namely the Shockley surface states (SSS), associated with the semi-infinite surface of a disordered alloy. (For a general review see, e.g., Inglesfield (1982).) Specific results for the low-index faces of Cu and Cu-based solid solutions with polyvalent impurities Zn, Al, and Ge are presented and discussed.

Our formal approach is to employ the Green function matching method used extensively by Inglesfield and co-workers (Inglesfield (1982) and references therein; for a general discussion of the method see Garcia-Moliner and Flores (1979)) in a number of surface related problems, to construct the average Green function for the semi-infinite alloy by matching the vacuum and bulk Green functions on the bounding surface. The bulk Green function is obtained on the basis of the Korringa–Kohn–Rostoker

† Permanent address: Physics Department, Indian Institute of Technology, Kanpur, India.

0953-8984/91/070801+12$03.50

coherent potential approximation (KKR-CPA) scheme for treating a randomly disordered alloy. (For a review and further references see: Bansil 1987, Stocks and Winter 1984, Ehrenreich and Schwartz 1976.) The presence of the surface is modelled as an abrupt potential step. These approximations obviously imply a rather idealized model of a surface. Nevertheless, such an approach has yielded reasonable results in describing aspects of the surface electronic structure in several cases of pure metals and disordered alloys. (See reviews by Inglesfield 1982, Jordan and Durham 1989.)

Concerning related work, the Green function matching of the sort invoked in the present study is presumably implicit in the formalism of Durham and co-workers (Durham 1984) who have considered angle-resolved photoemission intensities in disordered alloys based on the one-step model of Pendry (1976); these authors have in particular calculated SSS in CuNi(111) and CuPd(111) binary alloys (Jordan and Durham 1989). We note also some tight-binding model Hamiltonian work in connection with surface states in alloys. (Berk 1975, Ishida *et al* 1976, Velicky and Kudrnosky 1977, Wysokinski *et al* 1980, Bullet 1982.)

An outline of this article is as follows. These introductory remarks are followed in section 2 by a summary of the formalism used. Only the briefest presentation of the formalism is given in order to enable us to state clearly the approximations invoked and the equations used in the computations; the general aspects of the Green function matching method and the multiple scattering theory techniques have been described extensively in the literature. An explicit secular equation for the SSS-bands in a disordered alloy is derived. Section 3 gives details of muffin-tin potentials and other model parameters used in the calculations, and presents and discusses the binding energies and disorder induced smearings of the $\bar{Y}$-centred SSS on (110) surface and the $\bar{\Gamma}$-centred SSS on the (111) surface of Cu and Cu-based solid solution $Cu_{90}Al_{10}$, $Cu_{70}Zn_{30}$, and $Cu_{90}Ge_{10}$. The theoretical predictions are compared with the measurements in $Cu_{90}Al_{10}$ where corresponding angle-resolved photoemission results are available†. The concluding discussion in section 4 comments further on the limitations of our model, and gives a summary of our results.

2. Theoretical formulation

2.1. General equations

An outline of the Green function matching approach (Inglesfield 1982) is as follows. Consider two regions I and II, with potentials V_I and V_{II} respectively, separated by the surface S. The Green functions G_I and G_{II} for the two regions are given by the equations

$$(-\nabla^2 + V_I(r) - E)G_I(r, r') = -\delta(r, r') \tag{1}$$

$$(-\nabla^2 + V_{II}(r) - E)G_{II}(r, r') = -\delta(r, r') . \tag{2}$$

The Green function G for the combined system I + II satisfies

$$(-\nabla^2 + V(r) - E)G(r, r') = -\delta(r, r') \tag{3}$$

† The present $Cu_{90}Al_{10}$ alloy results were presented by Serageldin *et al* (1990).

where $V = V_{\rm I}$ when r is in region I, and $V = V_{\rm II}$ when r is in region II. Multiplying equation (3) by $G_{\rm I}$ and (1) by G, subtracting, and integrating over the volume of region I, upon using Green's theorem yields

$$G(r,r') = G_{\rm I}(r,r') - \int_S {\rm d}^2 r_s \left(G_{\rm I}(r,r_s)\frac{\partial G(r_s,r')}{\partial n_s} - \frac{\partial G_{\rm I}(r,r_s)}{\partial n_s} G(r_s,r') \right) \tag{4}$$

for r, r' in region I, and

$$G(r,r') = \int_S {\rm d}^2 r_s \left(G_{\rm II}(r,r_s)\frac{\partial G(r_s,r')}{\partial n_s} - \frac{\partial G_{\rm II}(r,r_s)}{\partial n_s} G(r_s,r') \right) \tag{5}$$

for r in region II and r' in region I. Here $\partial/\partial n_s$ denotes the normal derivative outward from I. Setting $r = r_s$ in equations (4) and (5) yields two simultaneous equations that can be solved for the surface values $G(r_s,r')$ and $\partial G(r_s,r')/\partial n_s$ by expanding these quantities in terms of an appropriate complete set of functions. $G(r,r')$ is then determined uniquely for all r and r' from the surface values of G via equations (4) and (5).

2.2. Bulk alloy and free-electron Green functions

In order to treat the ideal semi-infinite surface of a disordered alloy, we take $G_{\rm I}$ to be the bulk KKR-CPA Green function G_a, and $G_{\rm II}$ to be the free electron Green function G_0. For simplicity, the bulk alloy potential is assumed to extend right up to the surface, where it abruptly changes to the vacuum potential with the step V_0. The relevant form of G_a for the random binary alloy $\rm A_x B_y$ (with $y \equiv 1 - x$) of non-overlapping muffin-tin potentials (radius R_m) is well known (see Stocks and Winter 1984, Bansil 1987) and may be written in terms of the regular and irregular solutions $R_l^{A(B)}$ and $\tilde{R}_l^{A(B)}$ of the radial Schrödinger equation in the A(B) muffin-tin sphere, normalized such that outside the muffin-tin sphere (i.e. for $r \geq R_m$)

$$R_l^{\rm A(B)}(r) = \eta_l(\kappa r) - \cot\delta_l^{\rm A(B)} j_l(\kappa r) \tag{6a}$$

$$\tilde{R}_l^{\rm A(B)}(r) = j_l(\kappa r)\,. \tag{6b}$$

Here $\delta_l^{\rm A(B)}$ are the phase-shifts associated with the A(B) potential evaluated at energy E and $\kappa \equiv \sqrt{E}$. η_l and j_l are the spherical Neumann and Bessel functions respectively. The Green function $G_a^{nn}(r,r')$ when r and r' both lie in the nth cell is given by

$$G_a^{nn}(r,r') = \kappa \sum_L Y_L(\hat{r}) \sum_i c_i [\kappa R_l^i(r) C_L^i R_l^i(r') - R_l^i(r)\tilde{R}_l^i(r')] Y_L(\hat{r}')\,. \tag{7}$$

The index i runs over atomic species, with $c_{\rm A} = x$ and $c_{\rm B} = y$. $Y_L(\hat{r})$ are real spherical harmonics, and

$$C_L^{\rm A(B)} = -D_L^{\rm A(B)} T_{LL}^{00} \tag{8}$$

where

$$D_L^{\rm A(B)} = \{1 + [(\tau_l^{\rm A(B)})^{-1} - (\tau_L^{\rm CPA})^{-1}] T_{LL}^{00}\}^{-1}\,. \tag{9}$$

Here $T^{nm}_{LL'}$ are the energy-shell matrix elements of the KKR-CPA path operator, $\tau_l^{A(B)}$ and τ_L^{CPA} are on the energy-shell matrix elements of the t-matrices for atom A(B) and the CPA effective atom, respectively. The Green function $G_a^{nm}(r, r')$ for the case when r and r' are in different unit cells, with r lying in the nth cell and r' in the mth cell is given by

$$G_a^{nm}(r, r') = \kappa^2 \sum_{LL'} Y_L(\hat{r}) \left(\sum_{ij} c_i c_j R_l^i(r) P^{ij}_{LL'}(n-m) R_l^j(r') \right) Y_{L'}(\hat{r}') \tag{10}$$

where

$$P^{ij}_{LL'}(n-m) = D^i_L T^{nm}_{LL'} D^j_{L'}. \tag{11}$$

The symmetry of the semi-infinite system can be exploited by considering suitable periodic Green functions, rather than the functions G_a and G_0. For this purpose we define partial Fourier transforms $\tilde{G}_{aK}$ and $\tilde{G}_{0K}$ for a wavevector K parallel to the surface Brillouin zone (SBZ), where

$$\tilde{G}_{aK}(r, r') = \sum_m G_a(r, r' - R^s_m) \exp(-\mathrm{i} K \cdot R^s_m) \tag{12}$$

with a similar expression for $\tilde{G}_{0K}$. Here the summation extends over the N_s vectors $\{R^s_m\}$ of the surface lattice. $\tilde{G}_{aK}$ can be expressed in terms of the Fourier transform

$$\hat{G}_{ak}(r, r') = \sum_m G_a(r, r' - R_m) \exp(-\mathrm{i} k \cdot R_m) \tag{13}$$

of the bulk Green function, where the sum runs over the N lattice points $\{R_m\}$, and k is a Bloch waveector. The relation between $\tilde{G}_{aK}$ and $\hat{G}_{ak}$ is

$$\tilde{G}_{aK}(r, r') = \frac{d}{2\pi} \int_{-\pi/d}^{\pi/d} \mathrm{d}k_\perp \, \hat{G}_{a(K, k_\perp)}(r, r') \tag{14}$$

where d is the interplanar distance; K and $k_\perp$ are the parallel and normal components of k respectively.

We now introduce the angular momentum representation

$$\tilde{G}_{aK}(r, r') = \sum_{LL'} \tilde{\mathcal{G}}_{aK, LL'}(r, r') Y_L(\hat{r}) Y_{L'}(\hat{r}'). \tag{15}$$

An explicit formula for the coefficients $\tilde{\mathcal{G}}_{aK,LL'}$ is obtained straightforwardly by using equations (7)–(14). The results is

$$\tilde{\mathcal{G}}_{aK,LL'}(r, r') = \left(\kappa \sum_i c_i [\kappa R_l^i(r) C^i_L R_l^i(r') - R_l^i(r) \tilde{R}_l^i(r')] \delta_{LL'} \right) + \kappa^2 \sum_{ij} c_i c_j R_l^i(r) \tilde{P}^{ij}_{LL'}(K) R_l^j(r') \tag{16}$$

where we have defined

$$\tilde{P}^{ij}_{LL'}(K) = D^i_L\left(\frac{d}{\pi}\int_{-\pi/d}^{\pi/d} \mathrm{d}k_\perp\, \Gamma^{\mathrm{CPA}}_{LL'}(E;K,k_\perp)\right) D^j_{L'} \tag{17}$$

$$\begin{aligned}\Gamma^{\mathrm{CPA}}_{LL'}(E,\boldsymbol{k}) &= \sum_{m\neq 0} T^{0m}_{LL'}\exp(-\mathrm{i}\boldsymbol{k}\cdot\boldsymbol{R}_m) + T^{00}_{LL'}\delta_{LL'} \\ &= [(\tau^{\mathrm{CPA}}_L)^{-1}\delta_{LL'} - B(\boldsymbol{k},E)_{LL'}]^{-1} + T^{00}_{LL'}\delta_{LL'}.\end{aligned} \tag{18}$$

Here $B(\boldsymbol{k},E)$ is the matrix of the familiar KKR structure constants. The angular momentum decomposition of the free electron Green function $\tilde{G}_{0K}(\boldsymbol{r},\boldsymbol{r}')$ is obtained similarly. Thus we have

$$\tilde{G}_{0K}(\boldsymbol{r},\boldsymbol{r}') = \sum_{LL'}\tilde{\mathcal{G}}_{0K,LL'}(r,r')Y_L(\hat{r})Y_{L'}(\hat{r}') \tag{19}$$

with

$$\tilde{\mathcal{G}}_{0K,LL'}(r,r') = -\gamma j_l(\mathrm{i}\gamma r_<)h^{(1)}_l(\mathrm{i}\gamma r_>)\delta_{LL'} + \mathcal{D}^{L''}_{LL'}j_l(\mathrm{i}\gamma r)j_{l'}(\mathrm{i}\gamma r') \tag{20}$$

where

$$\mathcal{D}^{L''}_{LL'} = 4\pi\mathrm{i}^{l-l'}\sum_{L''}\mathrm{i}^{-l''}\mathcal{N}^{L''}_{LL'}[-\gamma\sum_j h_{l''}(\mathrm{i}\gamma R^i_j)\exp(\mathrm{i}K\cdot R^i_j)Y_{L''}(\hat{R}_j)] \tag{21}$$

with $\gamma^2 = V_0 - E$. $-\gamma^2$ is the electron energy with respect to the vacuum zero and

$$\mathcal{N}^{L''}_{LL'} = \int \mathrm{d}\Omega\, Y_L(\Omega)Y_{L'}(\Omega)Y_{L''}(\Omega) \tag{22}$$

are the Gaunt numbers.

The implementation of the preceding formalism is simplified if one uses Green functions $\tilde{G}^{\mathrm{WS}}_{aK}$ and $\tilde{G}^{\mathrm{WS}}_{oK}$ (rather than $\tilde{G}_{aK}$ and $\tilde{G}_{0K}$) which satisfy Neumann-type boundary conditions at the matching surface, i.e.

$$\frac{\partial\tilde{G}^{\mathrm{WS}}_{aK}}{\partial n_s} = \frac{\partial\tilde{G}^{\mathrm{WS}}_{oK}}{\partial n_s} = 0. \tag{23}$$

Such Green functions are easily constructed from $\tilde{G}_{aK}$ and $\tilde{G}_{0K}$ and their derivatives. The spherical harmonic expansions for $\tilde{G}^{\mathrm{WS}}_{aK}$ and $\tilde{G}^{\mathrm{WS}}_{0K}$ are given by

$$\tilde{\mathcal{G}}^{\mathrm{WS}}_{aK} = (1 - R_s^2\tilde{\mathcal{G}}'_{aK}M)^{-1}\tilde{\mathcal{G}}_{aK} \tag{24}$$

$$\tilde{\mathcal{G}}^{\mathrm{WS}}_{oK} = (1 + R_s^2\tilde{\mathcal{G}}'_{oK}M)^{-1}\tilde{\mathcal{G}}_{oK} \tag{25}$$

where $\tilde{\mathcal{G}}_{aK}$ and $\tilde{\mathcal{G}}_{0K}$ are the spherical harmonics expansions of $\tilde{G}_{aK}$ and $\tilde{G}_{0K}$ respectively over a WS sphere of radius R_s, $\tilde{\mathcal{G}}'_{aK}$ and $\tilde{\mathcal{G}}'_{0K}$ are the corresponding derivatives, and

$$M_{LL'} = \int_S Y_L(\hat{R}_s)Y_{L'}(\hat{R}_s)\,\mathrm{d}\Omega \tag{26}$$

is a matrix which involves an integral of the spherical harmonics over the matching surface S.

2.3. Green function for the semi-infinite alloy surface

The Green function $\tilde{G}_K(r,r')$ for the combined system (defined in a manner analogous to equation (12)) can be obtained in terms of $\tilde{G}_{aK}^{WS}$ and $\tilde{G}_{0K}^{WS}$ by using the matching conditions (4) and (5). Hereafter, following Inglesfield (1978; such an approximation is commonly invoked in the theory of muffin-tin systems) we will approximate the unit cell by a Wigner-Seitz (WS) sphere. The matching surface then becomes part of the WS sphere surface in the shape of a spherical 'cap'. We thus have

$$\tilde{G}_K(r,r') = \tilde{G}_{aK}^{WS}(r,r') - \int_S d^2r_s\, \tilde{G}_{aK}^{WS}(r,r_s)\frac{\partial \tilde{G}_K(r_s,r')}{\partial n_s} \tag{27}$$

for r and r' inside the WS sphere, and

$$\tilde{G}_K(r,r') = \int_S d^2r_s\, \tilde{G}_{oK}^{WS}(r,r'_s)\frac{\partial \tilde{G}_K(r_s,r')}{\partial n_s} \tag{28}$$

when r' lies in the alloy and r in the vacuum. Using spherical harmonic expansions for $\tilde{G}_K$, $\tilde{G}_a^{WS}$, and $\tilde{G}_0^{WS}$, and putting $r = R_s$ in equations (27) and (28), we get

$$\tilde{\mathcal{G}}_{K,LL'}(R_s,r') = \tilde{\mathcal{G}}_{aK,LL'}^{WS}(R_s,r') - R_s^2 \sum_{L''L'''} \tilde{\mathcal{G}}_{aK,LL''}^{WS}(R_s,R_s)M_{L''L'''}\tilde{\mathcal{G}}'_{K,L'''L'}(R_s,r') \tag{29}$$

$$\tilde{\mathcal{G}}_{K,LL'}(R_s,r') = R_s^2 \sum_{L''L'''} \tilde{\mathcal{G}}_{0K,LL''}^{WS}(R_s,R_s)M_{L''L'''}\tilde{\mathcal{G}}'_{K,L'''L'}(R_s,r'). \tag{30}$$

Equations (29) and (30) may be written in a compact matrix notation as

$$\tilde{\mathcal{G}}_K = \tilde{\mathcal{G}}_{aK}^{WS} - R_s^2\tilde{\mathcal{G}}_{aK}^{WS}M\tilde{\mathcal{G}}'_K \tag{31a}$$

$$\tilde{\mathcal{G}}_K = R_s^2\tilde{\mathcal{G}}_{0K}^{WS}M\tilde{\mathcal{G}}'_K\,. \tag{31b}$$

Solving for the derivative, we obtain

$$\tilde{\mathcal{G}}'_K = (R_s^2M)^{-1}[\tilde{\mathcal{G}}_{0K}^{WS} + \tilde{\mathcal{G}}_{aK}^{WS})]^{-1}\tilde{\mathcal{G}}_{aK}^{WS}\,. \tag{32}$$

Using (32) in (27), keeping definition (26) in mind, yields

$$\tilde{G}_K(r,r') = \tilde{G}_{aK}^{WS}(r,r') - \sum_{LL',L''L'''} \{\tilde{\mathcal{G}}_{aK,LL''}^{WS}(r,R_s)[\tilde{\mathcal{G}}_{0K}^{WS}(R_s,R_s)M + \tilde{\mathcal{G}}_{aK}^{WS}(R_s,R_s)M]^{-1}_{L''L'''}\tilde{\mathcal{G}}_{aK,L'''L'}^{WS}(R_s,r')Y_L(\hat{r})Y_{L'}(\hat{r}')\} \tag{33}$$

which is the desired expression for the semi-infinite alloy surface Green function in terms of the bulk KKR-CPA and the free electron Green functions.

2.4. Shockley-type surface state bands

The spectral density of states associated with the Green function $\tilde{G}_K(r, r')$ is

$$\varrho_{s,K}(E) = -\pi^{-1} \int_{WS} d^3r \, \mathrm{Im}\, \tilde{G}_K(r, r) = \varrho_{aK}(E) + \varrho_{bK}(E) \tag{34}$$

with the definitions

$$\varrho_{aK}(E) = -\pi^{-1} \int_{WS} d^3r \, \mathrm{Im}\, \tilde{G}^{WS}_{aK}(r, r) \tag{35}$$

$$\varrho_{bK}(E) = \pi^{-1} \sum_L \int_{WS} r^2 \, dr \, \mathrm{Im}\, [(\tilde{\mathcal{G}}^{WS}_{aK})^2(r, R_s)\{\tilde{\mathcal{G}}^{WS}_{0K}(R_s, R_s)M + \tilde{\mathcal{G}}^{WS}_{aK}(R_s, R_s)M\}^{-1}]_{LL} . \tag{36}$$

$\varrho_{sK}(E)$ is periodic in the SBZ and is the surface analogue of the Bloch spectral density in a bulk system. An integral of $\varrho_{sK}(E)$ over K yields the density of states. The contribution $\varrho_{aK}(E)$ on the right side of (34) arises from the bulk alloy Green function and gives the projection of the Bloch spectral density on to the SBZ. The second term $\varrho_{bK}(E)$ represents the surface contribution, giving additional peaks in the spectral density whenever

$$\|\tilde{\mathcal{G}}^{WS}_{surf}\| \equiv \|\tilde{\mathcal{G}}^{WS}_{oK} + \tilde{\mathcal{G}}^{WS}_{aK}\| = 0 . \tag{37}$$

This is the secular equation for obtaining Shockley state bands for the semi-infinite alloy surface. For a fixed K, the roots $E_n(K)$ of (37) will be real for a perfect crystal surface. In an alloy, on the other hand, (37) will in general yield 'complex' surface energy bands; the imaginary part of $E_n(K)$ represents the disorder scattering of surface states.

3. Results for low-index faces of Cu-based alloys

3.1. Computational details

The Cu, Al, Zn, and Ge muffin-tin potentials used in the present calculations are non-self-consistent and are based on the Herman–Skillman charge densities overlapped on the FCC Cu lattice of lattice constant 6.8309 au via the Mattheiss procedure. The specific muffin-tin potentials used in this work are identical to those employed in our previous studies of CuAl(Asonen *et al* 1982), CuZn (Prasad *et al* 1981), and CuGe (Prasad and Bansil 1982, Bansil *et al* 1984) solid solutions, where they yield a reasonable accord with the corresponding bulk band structures deduced from angle-resolved photoemission and other experiments. In computing the Green function for the semi-infinite surface, the height of the surface step V_0 was chosen to reproduce the measured work function W from the calculated Fermi energy E_F using the relation, $V_0 = E_F + W$. In Cu, W for the (110) surface is 4.49 eV, and E_F is 8.40 eV, giving $V_0 = 12.9$ eV. The Shockley states discussed in this article were found to be quite insensitive to variations on the order of 0.1 eV in the value of the parameter V_0. Differences in the values of work function between various low-index faces of Cu, and between Cu and Cu-based alloys of present interest are generally less than a few

tenths of an eV, as are the differences in the Fermi energies between Cu and the alloys considered in this work. For this reason, we also used $V_0 = 12.9$ eV in the alloy surface calculations. For the results given below, the matching surface in all cases was taken to be the hemispherical upper portion of the WS sphere (radius 2.67 au). A number of other computations using larger, as well as smaller, values of the effective radius of the matching sphere surface were carried out in order to ascertain the effect of the position of the matching surface on the SSS energy. While the absolute values of the surface states do vary with these changes as expected, the relative shifts in the surface state positions upon alloying, our main focus in this article, were found to be quite insensitive to such variations in the parameters of the model potential.

The present computer codes were checked extensively in the limiting case of a pure metal where they reproduce the detailed results concerning the surface state position and the phase of the surface Green function in Ni(001) given by Inglesfield (1978) for the Wakoh (1965) Ni potential. Care is needed in evaluating the Green function expansion co-efficients $\tilde{G}_{aKLL'}$ (cf equation (16)) which in view of equations (17)–(18) involve integrals with a singular integrand in the pure-metal limit. We evaluated these integrals by adding a small imaginary part of $\approx 10^{-5}$ Ryd in energy; the accuracy of the results was however checked by test calculations with much smaller imaginary parts of energy. This procedure was also employed in obtaining the path operators T_{00} in Cu. The KKR-CPA scattering phase shifts in $Cu_{90}Al_{10}$, $Cu_{70}Zn_{30}$, and $Cu_{90}Ge_{10}$, and the path operators in Cu as well as the alloy were calculated over a fine (a few mRyd) mesh in energy in order to obtain the complex bulk energy bands in the alloy accurately in the energy region of the surface states.

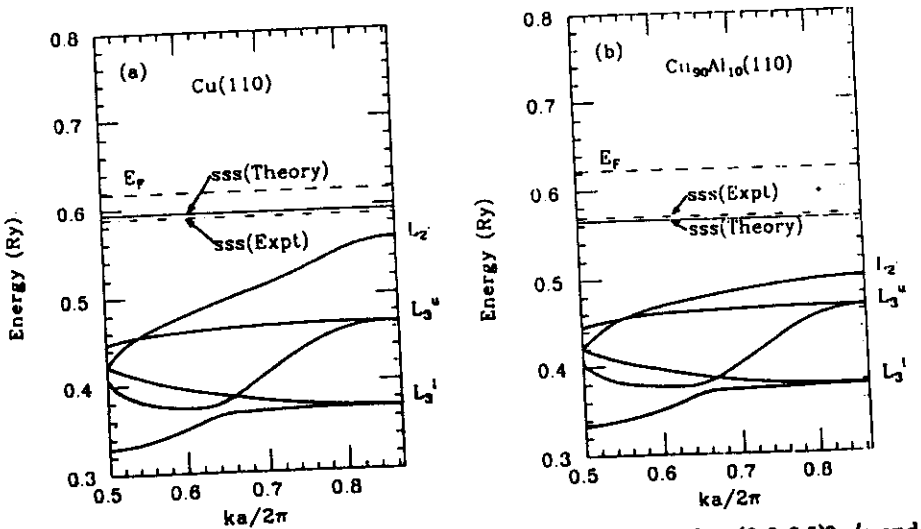

Figure 1. Bulk energy bands along the straight line joining $k = (0,0,0.5)2\pi/a$ and the symmetry point L in the Brillouin zone in: (*a*) Cu, and (*b*) $Cu_{90}Al_{10}$, relevant to the $\bar{\Gamma}$-centred Shockley state on the (110) surface. The bands in the alloy are of course complex, but are shown without their disorder induced widths for simplicity. The horizontal lines mark the positions of the Fermi energy E_F (broken line), the experimental values of binding energy of the Shockley surface states SSS (after Asonen *et al* (1982), chain line), and the theoretically predicted SSS binding energies (present work, full line).

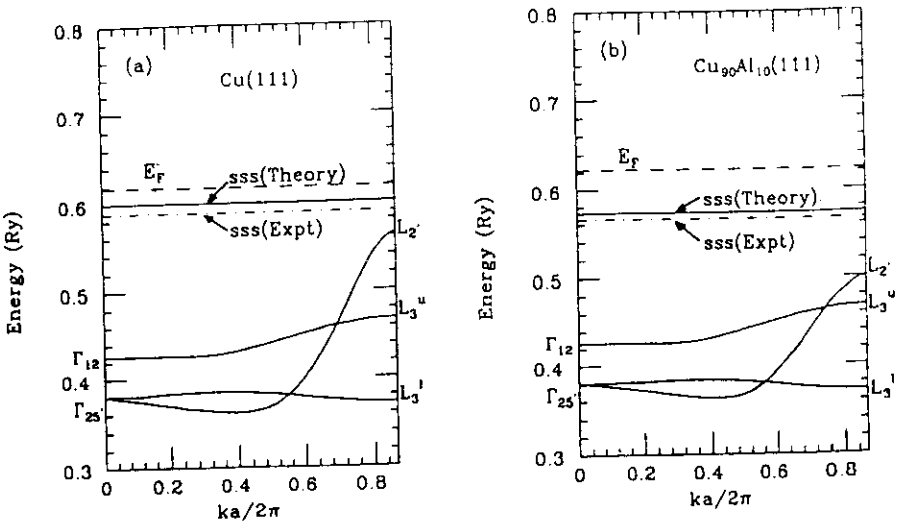

Figure 2. As figure 1 but for the $\bar{\Gamma}$-centred Shockley state on the (111) surface. The relevant bulk bands along the Γ–L symmetry direction are shown.

Our procedure for investigating surface states was as follows. The projected bulk bands at various K-points in the SBZ in Cu and the alloys (the energy bands in the disordered alloy are of course complex) were calculated. If a band gap existed in the projected bulk bands, we searched for possible Shockley state solutions of equation (37). Figure 1 is illustrative in this regard for the (110) surface; it shows bulk bands in Cu and $Cu_{90}Al_{10}$ for various $k_\perp$ values for a fixed $K_\parallel$ corresponding to the $\bar{Y}$ point in the SBZ. An sp-like band gap is seen to exist below E_F with an edge at the position of the $L_{2'}$ level in both Cu and $Cu_{90}Al_{10}$. By examining the zeros of the determinant of the surface matrix $\bar{G}^{WS}_{surf}$, we find SSS in Cu and $Cu_{90}Al_{10}$ at energies of 0.594 Ryd (0.33 eV below E_F) and 0.565 Ryd (0.79 eV below E_F) respectively. For the (111)-surface the bulk bands along the Γ–L direction were considered in order to study the $\bar{\Gamma}$-centred SSS; see figure 2 for the case of Cu and $Cu_{90}Al_{10}$. Here SSS were found at energies of 0.6 Ryd (0.25 eV below E_F) and 0.573 Ryd (0.68 eV below E_F) for Cu(111) and the alloy respectively. The disorder induced smearing of the surface states in alloys were estimated from the FWHM of the associated spectral peak, i.e. the integrand in equation (36). In this manner the low-index surfaces, (001), (110), and (111), were studied. No band gaps in the vicinity of the Fermi energy were found in the (001) case, and therefore a further investigation of the surface states was not pursued. The results for the (110) and (111) surfaces of Cu and Cu-based alloys are discussed below.

9.2. (110) and (111) surfaces of Cu, $Cu_{90}Al_{10}$, $Cu_{70}Zn_{30}$, and $Cu_{90}Ge_{10}$

The results for the $\bar{Y}$-centred SSS on the (110) surface and the $\bar{\Gamma}$-centred SSS on the (111) surface are summarized in tables 1 and 2 respectively. A direct comparison between theory and experiment is only possible in Cu and CuAl where these SSS have been observed in angle-resolved photoemission experiments (Asonen *et al* 1982); SSS were not observed in angle-resolved photoemission experiments on CuGe by Bansil *et al* (1984), most likely due to a poor surface quality. We are not aware of any corresponding experiments in CuZn alloys.

Table 1. The calculated binding energies, E_B (theory), and the associated disordered induced smearings (FWHM), δE (theory), for the $\bar{Y}$-centred Shockley state on the (110) surface in Cu and Cu-based alloys; the electron/atom ratios (e/a) for various alloys are given. The experimental values for Cu(110) and $Cu_{90}Al_{10}$(110) are from angle-resolved photoemission experiments of Asonen *et al* (1982); δE (experiment) is estimated from the observed widths of the SSS-feature in Cu and $Cu_{90}Al_{10}$; corresponding data for other alloys is not available. Theoretical and experimental values of shifts in the SSS-binding energy with respect to Cu are given in the fifth and sixth columns, respectively. Units are eV throughout. $\delta E_B^{theory} = (E_B^{alloy} - E_B^{Cu})_{theory}$, $\delta E_B^{expt} = (E_B^{alloy} - E_B^{Cu})_{expt}$.

	e/a	E_B^{theory}	E_B^{expt}	δE_B^{theory}	δE_B^{expt}	δE_{theory}	δE_{expt}
Cu	1.0	0.33	0.39				
$Cu_{90}Al_{10}$	1.2	0.79	0.74	0.46	0.35	0.45	0.36
$Cu_{70}Zn_{30}$	1.3	0.95		0.62		0.34	
$Cu_{90}Ge_{10}$	1.3	1.27		0.94		1.02	

Table 2. As table 1, but for the $\bar{\Gamma}$-centred SSS on the (111) surface. Units are eV throughout. $\delta E_B^{theory} = (E_B^{alloy} - E_B^{Cu})_{theory}$, $\delta E_B^{expt} = (E_B^{alloy} - E_B^{Cu})_{expt}$.

	e/a	E_B^{theory}	E_B^{expt}	δE_B^{theory}	δE_B^{expt}	δE_{theory}	δE_{expt}
Cu	1.0	0.25	0.40				
$Cu_{90}Al_{10}$	1.2	0.68	0.80	0.43	0.40	0.45	0.47
$Cu_{70}Zn_{30}$	1.3	0.85		0.60		0.34	
$Cu_{90}Ge_{10}$	1.3	1.16		0.91		0.99	

Tables 1 and 2 show reasonable agreement between theory and experiment in Cu and $Cu_{90}Al_{10}$. In particular, the theoretically predicted increase in binding energy of the SSS (the fifth column in each table) for both surfaces agrees with the corresponding measured increase in sign; the agreement with regard to the magnitude of the shift appears to be somewhat better for the (111) surface. Note, however, that the concentration of Al in the surface region in the experiments of Asonen *et al* (1982) was estimated to be about 13%; therefore the computed shifts should perhaps be proportionately scaled upwards. The theoretical values for the disordered induced smearing of the SSS in the alloy are in reasonable agreement with the measured increases (the eighth column in each table) in the line widths (FWHM) in the alloy compared with Cu. In general of course a surface state will be broadened in the real system by other mechanisms (e.g. surface imperfections) which are not included in the present theoretical estimate.

With reference to tables 1 and 2, we see that the theoretically predicted binding energy of the SSS increases with increasing electron/atom (e/a) ratios upon adding polyvalent impurities. A substantial solute dependence is nevertheless seen in that while e/a values for $Cu_{70}Zn_{30}$ and $Cu_{90}Ge_{10}$ are the same, the SSS parameters are quite different. Interestingly, the measured position of the SSS in the isoelectronic alloy CuAu is essentially unchanged from Cu, and in CuPd where electrons are depleted from the Fermi energy, the SSS is observed to move to *lower* binding energies with increasing *Pd* content in angle resolved photoemission experiments (Asonen *et al* 1985, Rao *et al* 1984); as noted above, the experimental SSS data in CuZn and CuGe is not available. However, angle-resolved photoemission calculations in Cu-rich CuNi(111)

and CuPd(111) yield an SSS feature at a lower binding energy (Jordan and Durham 1989). Physically, the (110) as well as the (111) SSS arises from bulk sp states in the vicinity of the $L_{2'}$ level. Figures 1 and 2 show that the $L_{2'}$ level is lowered substantially in the alloy, as the average potential in the unit cell becomes more attractive upon adding Al. (A similar effect occurs in CuZn and CuGe.) Therefore, the movement of the Shockley state to a higher binding energy in the alloy is to be expected qualitatively. The magnitude of the SSS shift however is generally less than that of the $L_{2'}$ level. This effect may be understood as being a consequence of the fact that a surface state is less sensitive than the bulk levels to potential changes in the bulk unit cell because the surface is surrounded by bulk atoms on only one side. In $Cu_{90}Al_{10}$, for example, the magnitude of the SSS-shift is only about half as much as that of the $L_{2'}$-level.

4. Discussion and conclusions

The use of non-self-consistent potentials in our work deserves further comment. In principle, the formalism can be developed to obtain a one-site restricted Green function (as opposed to the average Green function, equation (37)) for a single atom placed in the effective KKR-CPA medium in the presence of the surface. The charge density on any site may then be computed, providing a basis for a self-consistent scheme. In actual practice, however, such a procedure will be computationally quite demanding. One important consequence of the fact that we are using the same KKR-CPA scattering potential in all layers is that our model is unable to treat Tamm-type surface states; an extension of the formalism to allow a different potential in at least the topmost surface layer is necessary to obtain such surface states. On the other hand, Shockley states which arise mainly from the mere presence of the surface itself should not be very sensitive to details of the shape of the potential. These considerations provide some justification for assuming that the changes in the Shockley state characteristics upon alloying, our main motivation for this study, may be given reasonably within the framework of our model.

In conclusion, we have developed a Green function matching approach to study Shockley states on an ideal semi-infinite surface of a disordered alloy. Results for the low-index faces of Cu, $Cu_{90}Al_{10}$, $Cu_{70}Zn_{30}$, and $Cu_{90}Ge_{10}$ are presented. Reasonable agreement is found between theoretical predictions and the corresponding angle-resolved photoemission measurements with regard to the characteristic effects of alloying Al (i.e. changes in binding energy, and disorder induced smearing) on the Shockley states of Cu; it would be interesting to obtain experimental Shockley state paramters in CuZn and CuGe alloys. Our calculations indicate that the Shockley state binding energy will generally increase with an increasing electron/atom ratio

Acknowledgments

It is a pleasure to acknowledge important conversations with R S Rao, M Lindroos, and M Pessa, and the technical assistance of E Arola. This project is supported by the US DOE grant ER45223, and a travel grant under the US/Finland program of the NSF, and has benefitted from the allocation of supercomputer time on the ER-Cray at LLNL, and the San Diego Supercomputer Center. Acknowledgement is made to

the donors of the The Petroleum Research Fund, administered by the ACS, for partial support of this research.

References

Asonen H, Barnes C J, Pessa M, Rao R S and Bansil 1985 *Phys. Rev.* B 31 3245–50
Asonen H, Lindroos M, Pessa M, Prasad R, Rao R S and Bansil A 1982 *Phys. Rev.* B 25 7075–85
Bansil A 1987 *Electronic Band Structure and its Applications (Springer Lecture Notes in Physics 283)* ed M Yussouff (Berlin: Springer) p 273
Bansil A and Pessa M 1983 *Phys. Scr.* T 4 52–60
Bansil A, Rao R S, Prasad R, Asonen H and Pessa M 1984 *J. Phys. F: Met. Phys.* 14 273–9
Berk N F 1975 *Surf. Sci.* 48 289–303
Bullet D W 1982 *Solid State Commun.* 43 491–4
Durham P J 1984 *Electronic Structure of Complex Systems* ed P Phariseau and W M Temmerman (New York: Plenum) pp 709–60
Ehrenreich H and Schwartz L M 1976 *Solid State Physics* vol 31 (New York: Academic)
Garcia-Moliner F and Flores F 1979 *Introduction to the Theory of Solid Surfaces* (Cambridge: Cambridge University Press)
Heimann P, Hermann J, Miosga H and Neddermeyer H 1981 *Solid State Commun.* 37 519–22
Inglesfield J E 1978 *Surf. Sci.* 76 355–78
—— 1982 *Rep. Prog. Phys.* 45 223–84
Ishida I, Inoue N and Matsubara T 1976 *Prog. Theor. Phys.* 55 653–64
Jordan R G and Durham P J 1989 *Alloy Phase Stability (NATO ASI Series B 163)* ed G M Stocks and A Gonis (Amsterdam: Kluwer) pp 35–74
Jordan R G and Sohal G S 1982 *J. Phys. C: Solid State Phys.* 15 L663–7
Pendry J B 1976 *Surf. Sci.* 57 679–705
Pessa M, Asonen H, Rao R S, Prasad R and Bansil A 1981 *Phys. Rev. Lett.* 47 1223–6
Prasad R and Bansil A 1982 *Phys. Rev. Lett.* 48 113–6
Prasad R, Papadopoulus S C and Bansil A 1981 *Phys. Rev.* B 23 2607–13
Rao R S, A Bansil A, H Asonen and M Pessa 1984 *Phys. Rev.* B 29 1713–21
Serageldin A Y, Prasad R and Bansil A 1990 *Bull. Am. Phys. Soc.* 35 296
Stocks G M and Winter H 1984 *Electronic Structure of Complex Systems* ed P Phariseau and W M Temmerman (New York: Plenum) pp 463–85
Velicky B and Kundrmosky J 1977 *Surf. Sci.* 64 411–24
Wakoh S 1965 *J. Phys. Soc. Japan* 20 1894–1901
Wysokinski K I, Sobczuk H and Pilat M 1980 *Phys. Status Solidi* b 101 657–63